

On the “naturalness” of $d + ig$ superconductivity in Sr_2RuO_4

Andrew C. Yuan,¹ Erez Berg,² and Steven A. Kivelson¹

¹*Department of Physics, Stanford University, Stanford, CA 93405, USA*

²*Department of Condensed Matter Physics, Weizmann Institute of Science, Rehovot 7610001, Israel*

Many seemingly contradictory experimental findings concerning the superconducting state in Sr_2RuO_4 can be accounted for on the basis of a conjectured accidental degeneracy between two patterns of pairing that are unrelated to each other under the (D_{4h}) symmetry of the crystal: a $d_{x^2-y^2}$ -wave (B_{1g}) and a $g_{xy(x^2-y^2)}$ -wave (A_{2g}) superconducting state. In this paper, we propose a generic multi-band model in which the g -wave pairing involving the xz and yz orbitals arises from second-nearest-neighbor interactions. Even if time-reversal symmetry is broken - as in a $d + ig$ state - the superconductor remains gapless with a Bogoliubov Fermi surface that approximates a (vertical) line node. The model gives rise to a strain-dependent splitting between the critical temperature T_c and the time-reversal symmetry-breaking temperature T_{trsb} that is qualitatively similar to some of the experimental observations in Sr_2RuO_4 .

I. INTRODUCTION

For more than two decades, Sr_2RuO_4 was generally believed to be a chiral p -wave superconductor (SC) mainly due to a compelling narrative based on early experiments [1–5]. The extreme sensitivity of the superconducting state to impurities [6] unambiguously establishes that it is an unconventional SC, and various experiments confirm that the gap is nodal [7, 8]. However, recent nuclear magnetic resonance (NMR) experiments have seemingly ruled out triplet pairings of any sort [9–11].

Further constraints on the symmetry of the SC order can be inferred from a variety of experiments. Elasto-caloric data [12] obtained when the Fermi surface is tuned through a Lifshitz transition strongly suggests that the SC gap is non-vanishing at the Van Hove points. Moreover, ultrasound experiments, taken at face value, suggest a two-component order parameter with highly constrained symmetries [13, 14]: A discontinuity in the c_{66} shear modulus implies that the only possibilities consist of the innately two-dimensional irrep - $d_{xz} - d_{yz}$ (E_g) [15–19] - or an accidental degeneracy between two distinct one-dimensional irreps whose tensor product has B_{2g} symmetry, i.e., $d_{x^2-y^2}$ & g [20, 21] or s & d_{xy} [22, 23]. Evidence [24, 25] of time-reversal symmetry (TRS) breaking at or slightly below T_c provides further evidence of a two component order parameter.

That the Fermi surface of Sr_2RuO_4 is quasi-two-dimensional, i.e. it consists of three cylindrical sheets corresponding to the α , β , and γ bands, makes it seem unlikely that the SC order parameter has strong inter-layer pairing in the vertical z direction, which provides an additional strong reason to exclude the possibility of $d_{xz} - d_{yz}$ (E_g) pairing. This is further supported by the lack of a visible discontinuity in the $(c_{11} - c_{12})/2$ (B_{1g}) shear modulus [13].

Conversely, an accidental degeneracy between distinct irreps requires a certain degree of fine-tuning so that the critical temperature T_c is roughly equal to the TRS breaking temperature T_{trsb} , i.e., $T_c \approx T_{\text{trsb}}$. However, this requires only one-degree of fine tuning and thus could plausibly arise in a small subset of SC materials.

In our recent works [20, 21], we preferred the $d_{x^2-y^2} + ig$ pairing symmetry over the $s + id_{xy}$ wave, mainly due to experimental observations of line nodes in the SC gap function [7, 8, 26]. Indeed, in a single-band model, $d + ig$ pairing leaves symmetry protected line nodes along the diagonal directions (110), ($1\bar{1}0$), while $s + id_{xy}$ pairing would require an extra degree of fine tuning, i.e., a $s + id_{xy}$ -wave SC is generally fully gapped. However, a perturbative study of the effective interaction based on a “realistic” multi-band model of the electronic structure of Sr_2RuO_4 concluded that the leading instabilities are in the s and d_{xy} -channels [22, 23]; this result raises issues concerning the “naturalness” of the $d_{x^2-y^2} + ig$ SC state. In particular, within a single band on a square lattice, the pair-wave-function in a g -wave state vanishes at all distances shorter than 4th nearest-neighbors, and thus seemingly requires unnaturally long-range interactions.

To address this problem, we consider a generic multi-band microscopic BCS model in which the results follow largely from symmetry considerations. In this model, the g -wave always lives primarily on the α and β bands, which derive from the symmetry-related xz and yz Ru orbitals. =There are two reasons for this: (1) g -wave pairing is strongly disfavored in the xy -band in that the pair-wave-function vanishes where the density of states is largest in the vicinity of the Van Hove points. (2) Coupling between the xz and yz bands permits g -wave pairing to be induced by 2nd nearest-neighbor effective interactions, i.e. much shorter-range than is required in a single-band context. Conversely, the $d_{x^2-y^2}$ com-

ponent is strongest on the xy band.

As a consequence, the model readily accounts for the recently observed uniaxial stress dependence of the splitting of the critical temperature T_c from the time-reversal symmetry (TRS) breaking T_{trsb} [24]. As we show via microscopic BdG calculations (Fig. 3), application of uniaxial stress has little effect on T_c until it is sufficiently strong to trigger a sharply peaked enhancement close to the critical strain at which the xy -band crosses a van Hove point, leading to a divergent density of states (DOS) [12, 27, 28]. In contrast, across this Lifshitz transition, the xz and yz -bands are only slightly distorted (an asymmetry of $\sim 2\%$) [24] and thus the g -wave component of the order parameter is largely unaffected, resulting in a T_{trsb} that is only weakly strain dependent. (The strain dependence would be quite different for a putative $s+id_{xy}$ -wave state, in which both components sit on all bands.) Within our model, the approximate degeneracy between the d and g wave components persists in the presence of symmetry breaking shear strain. However, it is lifted by isotropic strain and leads to a linear increase in T_c ; this effect has not been detected in recent experiments [29]. How to reconcile this observation with our $d+ig$ proposal remains unresolved at present.

Regarding the nodal structure, we show that the symmetry-protected line nodes along the diagonal planes $(110), (1\bar{1}0)$ anticipated in the single-band model extend into Bogoliubov Fermi Surfaces (FS) in the general multi-band $d_{x^2-y^2} + ig$ state. The Bogoliubov FS are extended in the k_z direction, narrow in the in-plane k_x, k_y directions (in proportion to the spin-orbit coupling and the inter-layer hopping), and pinch into point nodes at the horizontal $k_z = 0, \pi$ planes, thereby forming a narrow elliptical FS. The pinching off at $k_z = 0, \pi$ is due to a combination of the mirror symmetries $\mathcal{M}_z : z \mapsto -z$ and $\mathcal{M}_{xy} : x \leftrightarrow y$. In practice, the Bogoliubov Fermi surfaces have a very small ‘‘Fermi energy’’, and are therefore expected to exhibit a behavior characteristic of line nodes (as is observed experimentally [7, 8, 26]), except at extremely low temperatures.

II. MICROSCOPIC ANALYSIS

A. Setup

Since Sr_2RuO_4 is quasi-two-dimensional, we shall consider an idealized 2D model with Bloch wave-vectors $\mathbf{k} = (k_x, k_y)$. The BCS Hamiltonian is

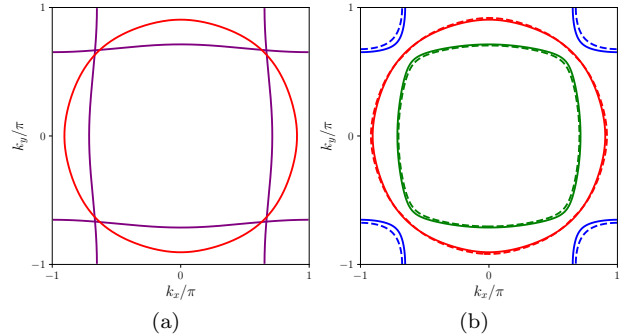


FIG. 1. (a) Fermi surfaces (FS) computed in the absence of hybridization and spin-orbit (SO) coupling. (b) FS including the effect of hybridization between the xz, yz bands but no SO (solid lines), and with both hybridization and SO (dashed lines). Here interplane dispersion is neglected; numerical parameters are given in Appendix (VA).

$$\mathcal{H} = \mathcal{H}_0 + \mathcal{H}_{\text{hybrid}} + \mathcal{H}_{\text{SO}} + \mathcal{H}_1 \quad (1)$$

$$\mathcal{H}_0 = \sum_{\mathbf{k}\nu s} \varepsilon_\nu(\mathbf{k}) \psi_{\nu s}^\dagger(\mathbf{k}) \psi_{\nu s}(\mathbf{k})$$

$$\mathcal{H}_{\text{hybrid}} = \sum_{\mathbf{k}s} \varepsilon_h(\mathbf{k}) (\psi_{xs}^\dagger(\mathbf{k}) \psi_{ys}(\mathbf{k}) + \text{h.c.})$$

$$\mathcal{H}_{\text{SO}} = \sum_{\mathbf{k}\nu\nu' s s'} \varepsilon_{\text{so}}(\mathbf{k}) \psi_{\nu s}^\dagger(\mathbf{k}) \psi_{\nu' s'}(\mathbf{k}) \mathbf{l}_{\nu\nu'} \cdot \boldsymbol{\sigma}_{s s'}$$

$$\mathcal{H}_1 = \sum_{\mathbf{k}\nu} \left(\Delta_\nu(\mathbf{k}) \psi_{\nu\uparrow}^\dagger(\mathbf{k}) \psi_{\nu\downarrow}^\dagger(-\mathbf{k}) + \text{h.c.} \right) + \sum_{\mathbf{k}} \left(\Delta_h(\mathbf{k}) \psi_{x\uparrow}^\dagger(\mathbf{k}) \psi_{y\downarrow}^\dagger(-\mathbf{k}) + \text{h.c.} \right)$$

The first term \mathcal{H}_0 represents the dispersion of each orbital $\nu = x, y, z$ (for d_{xz}, d_{yz}, d_{xy} respectively), while the second term $\mathcal{H}_{\text{hybrid}}$ is the hybridization between the x and y bands and generates the α and β bands shown in Fig. 1, where $\varepsilon_h(\mathbf{k})$ represents the strength of hybridization between the x, y bands [30]. The third term represents the spin-orbit (SO) coupling where $\mathbf{l}_{\nu\nu'}^\mu = -i\epsilon_{\nu\nu'\mu}$. The specific parameterizations of $\varepsilon_\nu(\mathbf{k})$, $\varepsilon_h(\mathbf{k})$, and $\varepsilon_{\text{so}}(\mathbf{k})$ used in our calculations are given in the Appendix (VA).

For simplicity, we shall restrict our analysis to even parity \mathcal{P} (in the 3D sense) gap functions, $\Delta_{a,b}$. Since the BCS Hamiltonian \mathcal{H} preserves mirror symmetry \mathcal{M}_z (mapping $z \mapsto -z$), the general multi-band particle-hole space can be decomposed into the eigenspaces of $\mathcal{M}_z = \pm i$. More specifically, particle states ($x \uparrow, y \uparrow, z \downarrow$) and hole states ($x \downarrow, y \downarrow, z \uparrow$) form a complete basis for the eigenspace $\mathcal{M}_z = +i$, while particle states ($x \downarrow, y \downarrow, z \uparrow$) and hole states ($x \uparrow, y \uparrow, z \downarrow$) form

a complete basis for the eigenspace $\mathcal{M}_z = -i$. Furthermore, let \mathcal{C} denote particle-hole symmetry of \mathcal{H} so that $\mathcal{K} \equiv \mathcal{P}\mathcal{C}$ denotes a symmetry local in \mathbf{k} . Since \mathcal{K} is an anti-unitary map between the $\mathcal{M}_z = +i \leftrightarrow \mathcal{M}_z = -i$ eigenspaces, we see that the BCS Hamiltonian \mathcal{H} in the decoupled eigenspaces $\mathcal{M}_z = \pm i$ have the same energy levels. Therefore, in the normal state ($\Delta = 0$), despite the SO coupling, there are only three distinct Fermi surfaces as shown in Fig. 1b. In the SC state ($\Delta \neq 0$), although SO coupling in general mixes singlet pairing and triplet pairing, we shall restrict ourselves to the case where the gap function is predominantly of singlet pairing, so that we can treat the triplet component perturbatively. This implies that Δ has no off-diagonal components between the γ band (derived from the z -band) and the α and β -bands, i.e., $\Delta_{x,z} = \Delta_{y,z} = 0$, as evident from the decomposition into eigenspaces of $\mathcal{M}_z = \pm i$, and thus explains our notation in \mathcal{H}_1 in Eq. (1).

Equivalently, we can use the following Nambu spinors

$$\Psi_+^\dagger(\mathbf{k}) = \begin{bmatrix} \psi_{x\uparrow}^\dagger(\mathbf{k}) \\ \psi_{y\uparrow}^\dagger(\mathbf{k}) \\ \psi_{z\downarrow}^\dagger(\mathbf{k}) \\ \psi_{x\downarrow}(-\mathbf{k}) \\ \psi_{y\downarrow}(-\mathbf{k}) \\ -\psi_{z\uparrow}(-\mathbf{k}) \end{bmatrix}, \Psi_-^\dagger(\mathbf{k}) = \begin{bmatrix} \psi_{x\downarrow}(\mathbf{k}) \\ \psi_{y\downarrow}(\mathbf{k}) \\ \psi_{z\uparrow}(\mathbf{k}) \\ -\psi_{x\uparrow}^\dagger(-\mathbf{k}) \\ -\psi_{y\uparrow}^\dagger(-\mathbf{k}) \\ \psi_{z\downarrow}^\dagger(-\mathbf{k}) \end{bmatrix} \quad (2)$$

to rewrite the BCS Hamiltonian in the following block-matrix form

$$\mathcal{H} = \sum_{\mathbf{k}, a=\pm} \Psi_a^\dagger(\mathbf{k}) H_a(\mathbf{k}) \Psi_a(\mathbf{k}) \quad (3)$$

$$H_\pm(\mathbf{k}) = \begin{bmatrix} \hat{\varepsilon}_\pm(\mathbf{k}) & \hat{\Delta}(\mathbf{k}) \\ \hat{\Delta}^\dagger(\mathbf{k}) & -\hat{\varepsilon}_\pm(\mathbf{k}) \end{bmatrix}$$

$$\hat{\varepsilon}_\pm(\mathbf{k}) = \begin{bmatrix} \varepsilon_x & \varepsilon_h \mp i\varepsilon_{\text{so}} & \pm\varepsilon_{\text{so}} \\ \varepsilon_h \pm i\varepsilon_{\text{so}} & \varepsilon_y & -i\varepsilon_{\text{so}} \\ \pm\varepsilon_{\text{so}} & i\varepsilon_{\text{so}} & \varepsilon_z \end{bmatrix}$$

$$\hat{\Delta}(\mathbf{k}) = \begin{bmatrix} \Delta_x & \Delta_h & 0 \\ \Delta_h & \Delta_y & 0 \\ 0 & 0 & \Delta_z \end{bmatrix}$$

where we have left the \mathbf{k} -dependence implicit in the entries of $\hat{\varepsilon}(\mathbf{k})$, $\hat{\Delta}(\mathbf{k})$.

B. Symmetries of multi-orbital gap functions

In a multi-band system, the gap function is a matrix-valued function of \mathbf{k} , making the symmetry analysis slightly complicated. For the present problem, it is sufficient to consider the two-band case,

corresponding to pairing on the α and β bands. Here, for any even-parity one-dimensional irrep, the general $\Delta(\mathbf{k})$ is a symmetric matrix, and so can be expressed as a sum of Pauli matrices as,

$$\Delta(\mathbf{k}) = \Delta_0(\mathbf{k}) + \Delta_1(\mathbf{k})\sigma_1 + \Delta_3(\mathbf{k})\sigma_3 \quad (4)$$

where $\Delta_1(\mathbf{k}) \equiv \Delta_h(\mathbf{k})$ is used for notation consistency and $\Delta_j(\mathbf{k})$ are scalar functions of \mathbf{k} . Since the point-group transformations act on the orbital indices as well as on \mathbf{k} , each function $\Delta_j(\mathbf{k})$ must itself transform in a specified way, as tabulated in Table I. Here we use the notation $S(\mathbf{k})$, $D(\mathbf{k})$, $D'(\mathbf{k})$, and $G(\mathbf{k})$ to designate functions of \mathbf{k} that transform under the point group in the indicated fashion, i.e. as A_{1g} , B_{1g} , B_{2g} , and A_{2g} respectively. For example, from the table we see that in a state with overall g -wave symmetry, $\Delta_0(\mathbf{k}) = G(\mathbf{k})$, $\Delta_1(\mathbf{k}) = D(\mathbf{k})$ and $\Delta_3(\mathbf{k}) = D'(\mathbf{k})$.

Overall Symmetry	$\Delta_0(\mathbf{k})$	$\Delta_3(\mathbf{k})$	$\Delta_1(\mathbf{k})$	
(A_{1g})	s	$S(\mathbf{k})$	$D(\mathbf{k})$	$D'(\mathbf{k})$
(B_{1g})	$d_{x^2-y^2}$	$D(\mathbf{k})$	$S(\mathbf{k})$	$G(\mathbf{k})$
(A_{2g})	g	$G(\mathbf{k})$	$D'(\mathbf{k})$	$D(\mathbf{k})$
(B_{2g})	d_{xy}	$D'(\mathbf{k})$	$G(\mathbf{k})$	$S(\mathbf{k})$

TABLE I. Symmetry Decomposition of the gap matrix in the two-orbital basis of Eq. 4.

Finally, since on physical grounds, we plan to deal only with the case in which the effective interactions are short-ranged, it is convenient to express each of these gap functions as a sum of lattice harmonics, specified by their range (R) and their symmetry. The first few such harmonics for each relevant symmetry are shown in Table II, normalized via their squared integral (L^2 -norm). Thus, for example, we can express $D(\mathbf{k}) = \sum_R \Phi_D(R) d_R(\mathbf{k})$ where $|\Phi_D(R)|$ is the magnitude of the $d_{x^2-y^2}$ symmetry gap parameter for creating a Cooper pair of range R (where $R = 1$ indicates nearest-neighbor sites, $R = 2$ is next-nearest neighbor, etc.).

Lattice Harmonic	$R = 0$	$R = 1$	$R = 2$	
(A_{1g})	$s_R(\mathbf{k})$	1	$\cos k_x + \cos k_y$	$2 \cos k_x \cos k_y$
(B_{1g})	$d_R(\mathbf{k})$	0	$\cos k_x - \cos k_y$	0
(B_{2g})	$d'_R(\mathbf{k})$	0	0	$2 \sin k_x \sin k_y$

TABLE II. First three harmonics ($R \leq 2$) based on symmetry and normalized via their squared integral. The 0 implies that there does not exist such a symmetry component for the given range. We have omitted the $g_R(\mathbf{k})$ -wave since it does not appear until 4th nearest-neighbor interactions ($R = 4$).

It is important to note that while the first g -wave lattice harmonic, $g_4(\mathbf{k}) = 2\sqrt{2}[\cos(k_x) -$

$\cos(k_y)] \sin(k_x) \sin(k_y)$, involves pairing on 4th neighbor sites, in the two band case a state with $\Delta_3(\mathbf{k}) = \Phi_{D'}(2) d'_2(\mathbf{k})$ has g -wave symmetry while only involving 2nd neighbor pairing. Indeed, a state with $\Delta_1(\mathbf{k}) = \Phi_D(1) d_1(\mathbf{k})$ has g -wave symmetry involving only nearest-neighbor pairing. However, since the hybridization ε_h in the band-structure is generally small compared to the diagonal terms ε_x , ε_y , and ε_z , the off-diagonal components of the gap matrix Δ are typically small for reasons unrelated to their range.

C. Nodal structure

We now turn to the nodal structure of the $d + ig$ phase. Generally, time reversal symmetry is required in order to obtain stable point nodes in the spectrum of a two-dimensional superconductor (or line nodes in three dimensions) [31–34]. It may therefore seem surprising that the $d + ig$ phase, which breaks time reversal, possesses protected nodes. As we shall now show, in two dimensions, there are stable point nodes along the Brillouin zone diagonals, protected by a combination of inversion symmetry and mirror reflections with respect to the planes perpendicular to \hat{z} and to $\hat{x} \pm \hat{y}$. Taking the three-dimensional dispersion into account, the nodes expand into narrow surfaces of gapless Bogoliubov quasi-particles, that become “pinched” into points at the $k_z = 0$ and π planes. However, the radius of these “Bogoliubov Fermi surfaces” is small in proportion to the inter-plane hopping, the spin-orbit coupling, and the ratio of the gap to the Fermi energy. In Sr_2RuO_4 , it is therefore expected that the Bogoliubov Fermi surfaces will be very narrow, and the $d + ig$ phase will display properties characteristic of line nodes (such as a linear dependence of the density of states on energy) down to extremely low energies.

In the single band context, a g -wave gap function has line nodes along the (100), (001), (110), (110) directions, as illustrated by $g_4(\mathbf{k})$ above. It then may seem that a g -wave in the two-band system of the anticipated form $\Delta_{x/y}(\mathbf{k}) = \pm D'(\mathbf{k})$, has the potential problem of missing line nodes along the zone diagonals $k_x = \pm k_y$. However, in the first section (II C 1), we shall explicitly show that the mirror symmetries $\mathcal{M}_z : z \mapsto -z$ and $\mathcal{M}_{xy} : x \leftrightarrow y$ protects the point node \mathbf{k}_* of the singlet-pairing $d_{x^2-y^2} + ig$ state along the zone diagonals in the horizontal plane $k_z = 0, \pi$. In Sr_2RuO_4 , either finite hybridization $\varepsilon_h \geq |\Delta_3|$ between the x, y bands or general SOC ε_{so} can play a role in resolving the apparent conundrum.

In the second section (II C 2), we shall consider a general 3D BCS Hamiltonian $H'(\mathbf{k})$, where $\mathbf{k} = (k_x, k_y, k_z)$ denotes the 3D wave-vector, to include

variations away from the horizontal planes $k_z = 0, \pi$, but still preserves the mirror symmetries $\mathcal{M}_z, \mathcal{M}_{xy}$. We then sketch a rigorous argument showing that in the regime where $H'(\mathbf{k}) - H'(\mathbf{k}_*)$ is small, the point nodes of $H'(\mathbf{k})$ in the intersection of $k_z = 0, \pi$ and $k_x = \pm k_y$ are stable and extend into Bogoliubov FS near the diagonal plane $k_x = k_y$. We shall derive the statement in three incremental steps.

1. In the intersection $k_z = 0, \pi$ and $k_x = \pm k_y$, we shall show that the original point node \mathbf{k}_* is stable and maps to \mathbf{k}'_* .
2. Away from the horizontal planes $k_z \neq 0, \pi$ where \mathcal{M}_z breaks down, the point node \mathbf{k}'_* extend into line nodes within the diagonal planes $k_x = \pm k_y$.
3. Away from mirror symmetries, i.e., $k_z \neq 0, \pi$ and $k_x \neq \pm k_y$, a Bogoliubov FS is generated.

Clearly, since $H'(\mathbf{k})$ is only weakly dependent in k_z , the region where the stability argument remains valid extends far in the k_z direction and thus implies the existence of extended Bogoliubov FS near the diagonal planes $k_x = \pm k_y$. In fact, when further mirror symmetry breaking perturbations are included (such as mixed triplet pairings due to SO coupling), the third step above can be repeated to find that a Bogoliubov FS is generated in the vicinity of the original line node. The detailed proof is presented in Appendix (V B).

1. Existence of point nodes in $k_z = 0, \pi$

First consider the case where the multi-band gap matrix $\hat{\Delta}(\mathbf{k})$ preserves TRS. In this case, the single-particle BCS Hamiltonian $H(\mathbf{k})$ has a node at \mathbf{k} if and only if [33, 35]

$$\det[\hat{\varepsilon}(\mathbf{k}) + i\hat{\Delta}(\mathbf{k})] = 0 \quad (5)$$

In general, the determinant is complex \mathbb{C} and thus we require 2 equations to be satisfied simultaneously. For a 2D system (3D system at $k_z = 0, \pi$), this implies that only point nodes can exist. However, if there exists a line (plane) across which $\hat{\Delta}(\mathbf{k}) \mapsto -\hat{\Delta}(\mathbf{k})$ via reflection symmetry, e.g., $d_{x^2-y^2}$ - or g -wave across the diagonals (110), (110), then the determinant is reduced to being real, $\det(\hat{\varepsilon} + i\hat{\Delta}) = \det(\hat{\varepsilon} - i\hat{\Delta})$, so that only 1 equation needs to be satisfied, and thus a point node exists along the symmetry lines.

In the case where Sr_2RuO_4 is characterized by a TRS breaking $d_{x^2-y^2} + ig$ SC state, the symmetry relations from Table I tell us that the gap component Δ_3 is the only possible nonzero component along

the diagonal directions (110) , $(\bar{1}\bar{0})$. Therefore, by a $U(1)$ -gauge transformation local in \mathbf{k} , we can always map the TRS breaking BCS Hamiltonian $H(\mathbf{k})$ to one that preserves TRS. More explicitly, there exists a node along the diagonal $\mathbf{k} = (k_x, \pm k_x)$ if and only if

$$|\Delta_3(\mathbf{k})|^2 \varepsilon_z(k) + \det \hat{\varepsilon}(\mathbf{k}) = 0 \quad (6)$$

Along the diagonals, $\varepsilon_x = \varepsilon_y$. Hence, in the absence of SOC, $\varepsilon_{so} = 0$, the equation reduces to

$$|\Delta_3(\mathbf{k})|^2 = \varepsilon_h(\mathbf{k})^2 - \varepsilon_x(\mathbf{k})^2 \quad (7)$$

Since the gap function is usually the smallest scale in the system, the equation generally holds true at some point along the diagonals, near the intersection of the FS of the x, y bands, despite the fact that $\Delta_3 \neq 0$.

2. Stability of nodes for general k_z

Since we have shown the existence of point nodes in the $k_z = 0, \pi$ planes, we can introduce a perturbative argument to study the stability of nodes as we move away from the explicit solutions \mathbf{k}_* . More explicitly, we shall study the behavior of a general BCS Hamiltonian $H'(\mathbb{k})$ which still preserves the same mirror symmetries \mathcal{M}_{xy} along $k_x = k_y$ and \mathcal{M}_z at $k_z = 0, \pi$. It should be noted that \mathcal{M}_{xy} maps $\Delta'(\mathbb{k}) \mapsto -\Delta'(\mathbb{k})$ in the diagonal planes $k_x = k_y$, but since this is a global phase, we can perform a $U(1)$ -gauge transformation \mathcal{U} local in \mathbb{k} so that $\tilde{\mathcal{M}}_{xy} = \mathcal{U}\mathcal{M}_{xy}$ is a symmetry of the full BCS Hamiltonian $H'(\mathbb{k})$ when $k_x = k_y$.

Let us first consider the intersection of $k_z = 0, \pi$ and $k_x = k_y$ so that $H'(\mathbf{k})$ has symmetries $\mathcal{M}_z, \tilde{\mathcal{M}}_{xy}$ and $\mathcal{K} = \mathcal{PC}$ which denotes a combination of particle-hole symmetry and parity. This operator is local in \mathbf{k} . As before, we can decompose $H'(\mathbf{k})$ into the eigenspaces of $\mathcal{M}_z = \pm i$ and since \mathcal{K} commutes with \mathcal{M}_z , it is an anti-unitary map between the eigenspaces $\mathcal{M}_z = +i \leftrightarrow \mathcal{M}_z = -i$. Similarly, $\tilde{\mathcal{M}}_{xy}$ anti-commutes with \mathcal{M}_z and maps between the eigenspaces $\mathcal{M}_z = +i \leftrightarrow \mathcal{M}_z = -i$. Hence, $\mathcal{K}\tilde{\mathcal{M}}_{xy}$ is an anti-unitary symmetry within each eigenspace $\mathcal{M}_z = \pm i$ and thus $H'(\mathbf{k})$ must be at least 4-times degenerate at its nodal points, i.e., $\dim \ker H'(\mathbf{k}) \in 4\mathbb{N}$. In particular, $\ker H'(\mathbf{k})$ is spanned by the complete basis

$$\{\phi'(\mathbf{k})\} \equiv (\phi', \tilde{\mathcal{M}}_{xy}\phi', \mathcal{K}\phi', \mathcal{K}\tilde{\mathcal{M}}_{xy}\phi') \quad (8)$$

where $\phi'(\mathbf{k})$ is some zero mode of $H'(\mathbf{k})$ and we have left \mathbf{k} implicit in the entries. This implies that for small perturbations from the nodal point \mathbf{k}_* of the

unperturbed $H(\mathbf{k})$, i.e., $H'(\mathbf{k}) - H(\mathbf{k}_*)$ is small, the behavior of $H'(\mathbf{k})$ can be modeled exactly by an effective 2-band (**pseudospin**) Hamiltonian $H'_{\text{eff}}(\mathbf{k})$ with the complete basis $\{\phi'(\mathbf{k})\}$. Since the effective 2-band Hamiltonian $H'_{\text{eff}}(\mathbf{k})$ must also satisfy the same symmetries $\mathcal{M}_z, \tilde{\mathcal{M}}_{xy}, \mathcal{K}$, explicit calculations show that

$$H'_{\text{eff}}(\mathbf{k}) = \varepsilon'_0(\mathbf{k})\sigma_0 \otimes \tau_3, \quad \varepsilon'_0(\mathbf{k}) \in \mathbb{R} \quad (9)$$

Where τ, σ denote the Pauli matrices in particle-hole space and the effective pseudospin space ($\phi'(\mathbf{k}), \tilde{\mathcal{M}}_{xy}\phi'(\mathbf{k})$), respectively. It is then clear that even with small perturbations, the point node is still stable and must exist at some \mathbf{k}'_* in the intersection of horizontal and diagonal planes.

Away from the horizontal planes $k_z \neq 0, \pi$, but within the diagonal plane $k_x = k_y$, a similar argument can be repeated to show that the nodal behavior can be modeled exactly by an effective 2-band Hamiltonian $H'_{\text{eff}}(\mathbb{k})$ provided that $H'(\mathbb{k}) - H(\mathbf{k}_*)$ is small (e.g., when $H'(\mathbb{k})$ depends weakly on k_z). Using the symmetries $\tilde{\mathcal{M}}_{xy}, \mathcal{K}$, an explicit calculation shows that

$$H'_{\text{eff}}(\mathbb{k}) = (\varepsilon'_0(\mathbb{k})\sigma_0 + \varepsilon'_1(\mathbb{k})\sigma_1) \otimes \tau_3, \quad \varepsilon'_i(\mathbb{k}) \in \mathbb{R} \quad (10)$$

And thus $H'_{\text{eff}}(\mathbb{k})$ has a node if and only if $|\varepsilon'_0(\mathbb{k})| = |\varepsilon'_1(\mathbb{k})|$. Since \mathbb{k} is restricted to the 2D diagonal plane, this implies that two line nodes extend from \mathbf{k}'_* in the diagonal plane, and thus imply the possibility of a conic shape near the horizontal planes $k_z = 0, \pi$.

Away from mirror planes, i.e., $k_z \neq 0, \pi$ and $k_x \neq k_y$, a similar argument can be repeated. Since \mathcal{K} is still preserved, we find that the gap matrix must form a singlet with respect to the pseudospins, i.e., $\hat{\Delta}'(\mathbb{k}) = \Delta'(\mathbb{k})(i\sigma_2)$. This implies that the particle-hole dispersion relation $\hat{\varepsilon}'(\mathbb{k})$ can be unitarily transformed via any $SU(2)$ rotation in pseudospin space without affecting the gap function. Therefore, the effective 2-band Hamiltonian $H'_{\text{eff}}(\mathbb{k})$ can be unitarily transformed so that $\hat{\varepsilon}'(\mathbb{k})$ is diagonal with entries $\varepsilon'_{\pm}(\mathbb{k})$, i.e.,

$$H'_{\text{eff}}(\mathbb{k}) = \left(\begin{array}{c|c} \varepsilon'_+ & \Delta' \\ \hline \varepsilon'_- & -\Delta' \\ \hline -\Delta'^* & -\varepsilon'_+ \\ \hline \Delta'^* & -\varepsilon'_- \end{array} \right) \quad (11)$$

Where the \mathbb{k} -dependence of the entries $\varepsilon'_{\pm}(\mathbb{k}), \Delta'(\mathbb{k})$ are kept implicit, and the solid lines divide the particle/hole subspaces. Therefore, the effective Hamiltonian $H'_{\text{eff}}(\mathbb{k})$ has a zero mode if and only

$$|\Delta'(\mathbb{k})|^2 + \varepsilon'_+(\mathbb{k})\varepsilon'_-(\mathbb{k}) = 0 \quad (12)$$

In the absence of mirror symmetries and TRS, a small Zeeman-like splitting occurs in pseudospin space, i.e., $\varepsilon'_+(\mathbf{k}) \neq \varepsilon'_-(\mathbf{k})$, and thus a Bogoliubov FS is generated where Eq. (12) is satisfied.

III. NUMERICAL RESULTS

A. Setup

We consider an interaction of the form

$$\mathcal{V} = \frac{1}{2} \sum_{\mu\mu', \mathbf{k}\mathbf{k}'} V_{\mu\mu'}(\mathbf{k}-\mathbf{k}') P_{\mu}^{\dagger}(\mathbf{k}) P_{\mu'}(\mathbf{k}') \quad (13)$$

where $P_{\mu}(\mathbf{k}) = \psi_{\downarrow\mu}(-\mathbf{k})\psi_{\uparrow\mu}(\mathbf{k})$ annihilates a Cooper pair in band μ and $V_{\mu\mu'}(\mathbf{q})$ represents the interaction between bands μ, μ' . By construction, the form of $V_{\mu\mu'}(\mathbf{q})$ precludes interband pairing of the SC gap, i.e. the self-consistency equations imply $\Delta_h = 0$; a more general form of the interaction would generally lead to a small but non-zero Δ_h , but this would not change any of our findings qualitatively.

We shall take interactions that respect the lattice symmetries and have range $R \leq 2$ [36]:

$$V_{\mu\mu'}(\mathbf{q}) = \sum_{R=0,1,2} v_{\mu\mu'}(R) s_R(\mathbf{q}), \quad (14)$$

where s_R is given by the first row in Table II. It is then convenient to express V as a sum of terms of the form $c_a \psi_a(\mathbf{k})\psi_a(\mathbf{k}')$ where each $\psi_a(\mathbf{k})$ transforms according to one of the irreps of the point group. We leave the details of the decomposition in Appendix (VC). For completeness, the nonlinear gap equation is given here

$$\Delta_{\mu}(\mathbf{k}) = \sum_{\mu'\mathbf{k}'} V_{\mu\mu'}(\mathbf{k}-\mathbf{k}') \langle P_{\mu'}(\mathbf{k}') \rangle \quad (15)$$

where the expectation value $\langle \dots \rangle$ is taken with respect to the BCS Hamiltonian.

For simplicity, we will henceforth set the spin-orbitcoupling to zero, since (so long as it is not too large) it does not qualitatively affect the results. In particular, the Lifshitz transition occurs at \mathbf{k} -points $(\pi, 0)$, $(0, \pi)$, where the orbital character of each band is well-defined and thus the SO terms vanish in any case. In this limit, the 2-band system consisting of the α and β bands decouples from the γ band within the BCS Hamiltonian, though all three bands are still coupled via the interaction term \mathcal{V} in the nonlinear gap equation in Eq. (15). Using the fact that $SU(4)$ is the spin group of $SO(6)$, we provide an intuitive manner of diagonalizing the 4×4 BdG Hamiltonian involving the 2-band system, details of which are left in Appendix (VD).

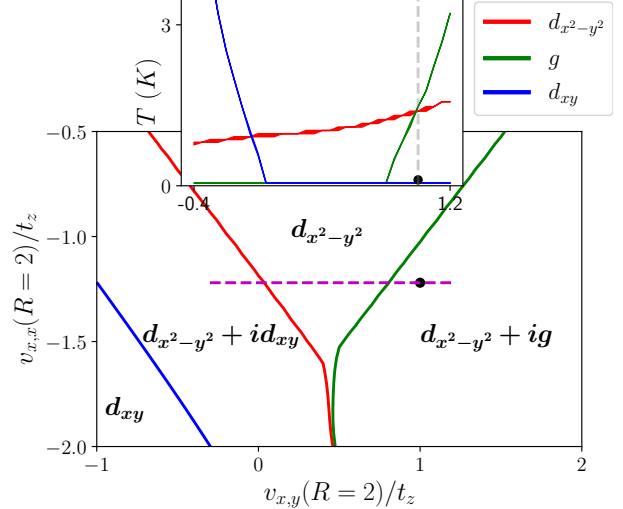


FIG. 2. Phase Diagram at $T = 0$ as a function of two interaction parameters: the inter-band 2nd neighbor interaction $v_{x,y}(R = 2)$ and the intra-band 2nd neighbor interaction $v_{x,x}(R = 2)$. The remaining interaction parameters (see Table. III) are fixed so that there exists a background $d_{x^2-y^2}$ wave even when $v_{x,y}(2) = v_{x,x}(2) = 0$. Solid lines are phase boundaries. The inset shows the thermal evolution of the critical temperatures T_c for each component ($d_{x^2-y^2}$, g , d_{xy} waves) along the cut through the phase diagram denoted by the dashed purple line. The black dot indicates the specific set of parameters (see Table. III) used in subsequent calculations, including those represented in Figs. 3 and 4.

Interaction v/t_z	$R = 0$	$R = 1$	$R = 2$
$v_{x,x}(R)$	7	-0.4	0.3
$v_{z,z}(R)$	5	-0.1	-1.2
$v_{x,y}(R)$	5	-0.1	1
$v_{x,z}(R)$	5	0.1	0.1

TABLE III. Specific parameters (in units of the nearest-neighbor hopping t_z on the γ band) chosen of the interaction term in Eq. (14) corresponding to the dot in Fig. 2. Note that in Fig. 2, only $v_{x,x}(2), v_{x,y}(2)$ were varied.

B. Zero temperature $T = 0$

Fig. 2 shows a cut through the $T = 0$ phase diagram in response to intra- and inter-band couplings, obtained by solving the self-consistent BCS equations described in Eq. (15). Indeed, since we are constructing overall g -waves using the anticipated form $\Delta_{x/y}(\mathbf{k}) = \pm D'(\mathbf{k})$ and $d'_R(\mathbf{k})$ is first nonzero for 2nd neighbor $R = 2$, there are exactly 2 parameters that can be tuned to generate d_{xy} - or g -wave symmetries, that is, the $R = 2$ inter- $v_{x,y}(2)$ and intra-band interactions $v_{x,x}(2)$, which correspond to the x, y axes in Fig. 2. The remaining interaction

parameters are fixed and given in Table III, tuned so that at $T = 0$ and $v_{x,x}(2) = v_{x,y}(2) = 0$, there exists a background $d_{x^2-y^2}$ -wave. Throughout, the preferred phase relation between the two components is such as to break time-reversal symmetry, i.e. $d_{x^2-y^2} \pm ig$ or $d_{x^2-y^2} \pm id_{xy}$.

In the vast parameter space of interactions, it is probably unsurprising that we can find regions in which the $d_{x^2-y^2}$ - and g -waves coexist. However, while in any single band problem, such coexistence regions are generically exceedingly narrow, here the coexistence region is large reflecting the fact that the two components live primarily on different bands, and so hardly compete with one another. In contrast, the accidental degeneracy between the $d_{x^2-y^2}$ and d_{xy} state is quickly destroyed by the preference for a pure d_{xy} wave as shown in Fig. 2. By tuning the x, y band interactions, the presence of a strong d_{xy} wave among the α, β -bands in general generates a nonzero component on the γ band and thus induces competition with the $d_{x^2-y^2}$ wave on the γ bands. Therefore, the system must exhibit a pure d_{xy} state in the limit of strong interactions favoring the d_{xy} wave. A similar logic would apply in the instance where the background state is an s -wave instead of a $d_{x^2-y^2}$ -wave.

Within the coexistence regions, the transition temperatures of the two orders are comparable, i.e., $T_c \sim T_{\text{trsb}}$. Indeed, in the inset graph in Fig. 2, we plot the onset temperature T_{onset} of each component ($d_{x^2-y^2}, g, d_{xy}$ waves) along the given cut (dashed purple line) in the phase diagram. As the secondary order component transitions from $d_{xy} \rightarrow g$ wave (left to right), the corresponding background $d_{x^2-y^2}$ wave has a slight increase in T_c .

C. Splitting of T_c, T_{trsb} with uniaxial stress

Let us tune the parameters to the dot in Fig. 2 so that the ground-state has $d_{x^2-y^2} \pm ig$ pairing and $T_c \approx T_{\text{trsb}}$ in the absence of strain. We model the effect of uniaxial stress (parametrized by ε_{xx}) by varying the band parameters in a manner consistent with experiment [12, 27] such that the γ -band crosses the van Hove point ($0, \pm\pi$) at $\varepsilon_{xx} \approx -0.44\%$ (details in Appendix (VE)). The α, β -bands are also distorted, but only slightly [27].

The resulting critical temperature for the d and g -components are given in Fig. 3. Due to symmetry breaking uniaxial stress, the point group symmetry D_{4h} is broken, while the subgroup D_{2h} is preserved. This implies that the $d_{x^2-y^2}$ component in general gains an s -wave component. Similarly, the g -wave should also gain a d_{xy} -wave component. However, our numerical calculations show that the

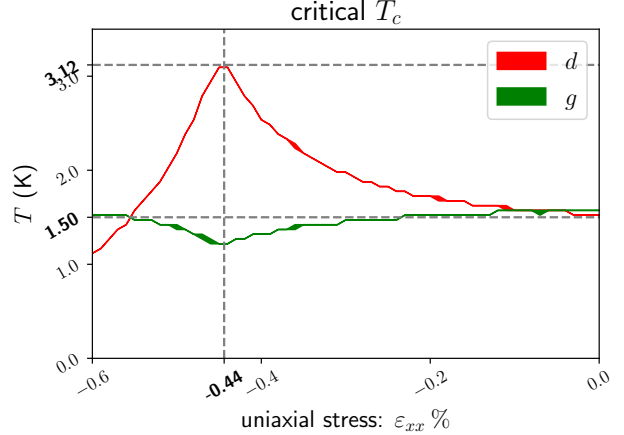


FIG. 3. Critical Temperatures. The red and green lines represent the critical temperatures of the d - and g -wave components. (The thickness denotes numerical uncertainty in the result based on calculations on a 3000^2 -site square lattice.) The Lifshitz transition occurs at a uniaxial stress $\varepsilon_{xx} \approx -0.44\%$.

additional d_{xy} is much smaller than the g -wave component. This is presumably due to the fact that the α, β -bands are minimally distorted in the presence of strain, while the strong d or $d + s$ -wave component on the γ -band suppresses any other symmetry component. Therefore, we label the corresponding symmetries as given in the legend of Fig. 3.

In the presence of small uniaxial stress $\varepsilon_{xx} \gtrsim -0.2\%$, away from the Lifshitz transition, the critical temperatures remain remarkably close to each other, and thus the accidentally degenerate $d + ig$ -state is stable when the DOS remains roughly constant. Near the van Hove point $\varepsilon_{xx} \approx -0.44\%$, the d -wave channel is enhanced causing the observed split in $T_c > T_{\text{trsb}}$. At a value of the strain somewhat beyond the van Hove point, $\varepsilon_{xx} \lesssim -0.5\%$, our calculations suggest that the g -wave component is first observed when entering superconductivity. However, note that in the context of SRO, there exists an observed competing spin-density-wave (SDW) [24] which is not incorporated in our calculations.

D. Response to pure B_2 and A_1 strain

We again tune the parameters to the dot in Fig. 2 so that the d, g waves are accidentally degenerate and investigate the response of our multi-band model to pure B_2 and pure A_1 strain. The resulting critical temperatures regarding the onset of d and g waves are shown in Fig. 4. In Fig. 4a, symmetry breaking B_2 strain is simulated by modifying the 2nd nearest neighbor ($R = 2$) hoppings in the normal state band structure (details in Appendix (VE)). In

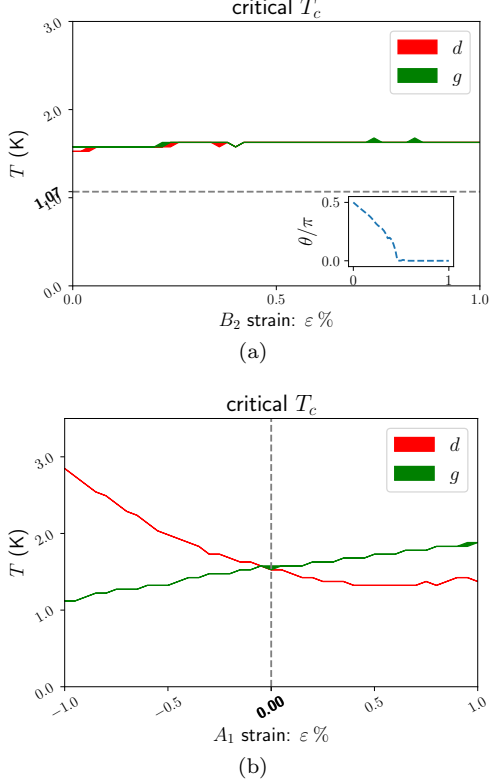


FIG. 4. The red and green lines represent the critical temperature T at which the d - and g -waves occur under (a) pure B_2 strain and (b) pure A_1 strain. The inset in subplot (a) shows the relative phase between the d and g -waves near T_c , i.e., along the horizontal dashed line in subplot (a).

this case, the critical temperatures remain remarkably close to each other even at large strain values (at which the relative phase between the d, g components is $\theta = 0$) and thus provides further evidence to the stability of the accidental degeneracy in the presence of strain. In Fig. 4b, we introduced pure A_1 strain by tuning the relative energies of the three bands so that the γ band is driven towards (away from) the Van Hove singularity for negative (positive) values ϵ , with the total density of electrons held fixed (see Appendix (V E)). This results in a cross over between the d, g waves, i.e., for $\epsilon < 0$ the d -wave is favored over the g wave and vice-versa, resulting in a kink-like feature in the overall T_c (maximum of the two lines in Fig. 4b) at $\epsilon = 0$. No such kink has been detected in experiments on SRO to date [29].

IV. SUMMARY

Although Sr_2RuO_4 would seem to be the ideal material to serve as the model system for uncon-

ventional superconductivity, given that its normal state is an extremely well characterized Fermi liquid, even the symmetries of the superconducting state has remained controversial [5]. Ultimately, this issue can only be settled by either reproducible phase-sensitive measurements, or by direct imaging (e.g. by angle-resolved photoemission or quasi-particle interference) of the gap structure on the Fermi surfaces. However, in the absence of these, further progress must rely on more indirect evidence based on comparisons between relatively robust aspects of theory and experimentally detected trends. Some of these aspects depend only on symmetry. However, while microscopic aspects of the problem are more difficult to access unambiguously, certain features, especially those that relate directly to qualitative aspects of the known band-structure, can be useful for the present purposes.

Here, we have analyzed a simple microscopic model with the band-structure of Sr_2RuO_4 and effective pairing interactions treated as phenomenological input. We have found several features of the solution of this problem that lend credence to the conjecture that the peculiar difficulty in settling the order parameter question arises from an accidental near-degeneracy between a $d_{x^2-y^2}$ -wave and g -wave pairing tendency. Specifically, we find the following suggestive results:

- It is sufficient to consider a model with relatively short-ranged pairing interactions - out to second neighbor distance. In common with many previous studies [37–40], we find that the generic result is that pairing is dominant either on the γ band or on the α and β bands. Thus, in any case, a certain degree of fine-tuning of the interactions is necessary to insure that the gap magnitude is comparable on all bands (as is experimentally established [41]).
- Under circumstances of near degeneracy, the $d_{x^2-y^2}$ -wave pairing occurs dominantly on the γ band and the g -wave on the α and β bands. Loosely, this near-degeneracy requires no more fine-tuning than is required to have comparable gaps on all bands.
- As a consequence, if the band-structure is tuned (for instance by uniaxial stress) such that the γ band approaches the nearby Van Hove point, this can significantly enhance the d -wave component of the order parameter, but has relatively little effect on the g -wave. (Generally, if two components coexist in the same bands, then whatever enhances one tends to suppress the other.)
- The existence of gapless (nodal) quasi-particles

is protected by symmetry, even if time-reversal symmetry is broken in a $d_{x^2-y^2} + ig$ state, so long as the (110) mirror symmetry of the crystal is unbroken.

While none of these results is sufficiently unique to serve as confirmation of the basic scenario, they serve to increase confidence in its “naturalness.”

Note added. During the preparation of the current manuscript, the following pre-print [42] appeared on arXiv, in which the authors stabilized a $d_{x^2-y^2} + ig$ state via introducing a 2nd nearest-neighbor term in the bare interaction. Although the calculation was done in the weak coupling limit in terms of RPA, it agrees with our proposal that a relatively short-

ranged model is sufficient to stabilize a g -wave component.

ACKNOWLEDGMENTS

SAK and AY were supported, in part, by NSF grant No. DMR-2000987 at Stanford. EB was supported by the European Research Council (ERC) under grant HQMAT (Grant Agreement No. 817799), the Israel-US Binational Science Foundation (BSF), and a Research grant from Irving and Cherna Moskowitz.

-
- [1] Andrew Peter Mackenzie and Yoshiteru Maeno, “The superconductivity of Sr_2RuO_4 and the physics of spin-triplet pairing,” *Reviews of Modern Physics* **75**, 657 (2003).
 - [2] Manfred Sigrist, “Review on the chiral p-wave phase of Sr_2RuO_4 ,” *Progress of Theoretical Physics Supplement* **160**, 1–14 (2005).
 - [3] Yoshiteru Maeno, Shunichiro Kittaka, Takuji Nomura, Shingo Yonezawa, and Kenji Ishida, “Evaluation of spin-triplet superconductivity in Sr_2RuO_4 ,” *Journal of the Physical Society of Japan* **81**, 011009 (2011).
 - [4] Catherine Kallin, “Chiral p-wave order in Sr_2RuO_4 ,” *Reports on Progress in Physics* **75**, 042501 (2012).
 - [5] Andrew P Mackenzie, Thomas Scaffidi, Clifford W Hicks, and Yoshiteru Maeno, “Even odder after twenty-three years: The superconducting order parameter puzzle of Sr_2RuO_4 ,” *npj Quantum Materials* **2**, 1–9 (2017).
 - [6] AP Mackenzie, RKW Haselwimmer, AW Tyler, GG Lonzarich, Y Mori, S Nishizaki, and Y Maeno, “Extremely strong dependence of superconductivity on disorder in Sr_2RuO_4 ,” *Physical review letters* **80**, 161 (1998).
 - [7] C Lupien, WA MacFarlane, Cyril Proust, Louis Taillefer, ZQ Mao, and Y Maeno, “Ultrasound attenuation in Sr_2RuO_4 : An angle-resolved study of the superconducting gap function,” *Physical review letters* **86**, 5986 (2001).
 - [8] I Bonalde, Brian D Yanoff, MB Salamon, DJ Van Harlingen, EME Chia, ZQ Mao, and Y Maeno, “Temperature dependence of the penetration depth in Sr_2RuO_4 : Evidence for nodes in the gap function,” *Physical review letters* **85**, 4775 (2000).
 - [9] Kenji Ishida, Masahiro Manago, Katsuki Kinjo, and Yoshiteru Maeno, “Reduction of the 17O Knight shift in the superconducting state and the heat-up effect by NMR pulses on Sr_2RuO_4 ,” *Journal of the Physical Society of Japan* **89**, 034712 (2020).
 - [10] Andrej Pustogow, Yongkang Luo, Aaron Chronister, Y-S Su, DA Sokolov, Fabian Jerzembeck, Andrew Peter Mackenzie, Clifford William Hicks, Naoki Kikugawa, Srinivas Raghunath, *et al.*, “Constraints on the superconducting order parameter in Sr_2RuO_4 from oxygen-17 nuclear magnetic resonance,” *Nature* **574**, 72–75 (2019).
 - [11] Aaron Chronister, Andrej Pustogow, Naoki Kikugawa, Dmitry A Sokolov, Fabian Jerzembeck, Clifford W Hicks, Andrew P Mackenzie, Eric D Bauer, and Stuart E Brown, “Evidence for even parity unconventional superconductivity in Sr_2RuO_4 ,” arXiv preprint arXiv:2007.13730 (2020).
 - [12] You-Sheng Li, Markus Garst, Jörg Schmalian, Naoki Kikugawa, Dmitry A Sokolov, Clifford W Hicks, Fabian Jerzembeck, Matthias S Ikeda, Andreas W Rost, Michael Nicklas, *et al.*, “Elastocaloric determination of the phase diagram of $\text{Sr}_{1-x}\text{RuO}_4$,” arXiv preprint arXiv:2201.04147 (2022).
 - [13] Sayak Ghosh, Arkady Shekhter, F Jerzembeck, N Kikugawa, Dmitry A Sokolov, Manuel Brando, AP Mackenzie, Clifford W Hicks, and BJ Ramshaw, “Thermodynamic evidence for a two-component superconducting order parameter in Sr_2RuO_4 ,” *Nature Physics* **17**, 199–204 (2021).
 - [14] Siham Benhabib, C Lupien, I Paul, L Berges, M Dion, M Nardone, A Zitouni, ZQ Mao, Y Maeno, A Georges, *et al.*, “Ultrasound evidence for a two-component superconducting order parameter in Sr_2RuO_4 ,” *Nature physics* **17**, 194–198 (2021).
 - [15] Igor Žutić and Igor Mazin, “Phase-sensitive tests of the pairing state symmetry in Sr_2RuO_4 ,” *Physical review letters* **95**, 217004 (2005).
 - [16] Sophie Beck, Alexander Hampel, Manuel Zingl, Carsten Timm, and Aline Ramires, “Effects of strain in multiorbital superconductors: The case of Sr_2RuO_4 ,” *Phys. Rev. Research* **4**, 023060 (2022).
 - [17] Aline Ramires, “Nodal gaps from local interactions in Sr_2RuO_4 ,” in *Journal of Physics: Conference Series*, Vol. 2164 (IOP Publishing, 2022) p. 012002.
 - [18] Han Gyeol Suh, Henri Menke, PMR Brydon,

- Carsten Timm, Aline Ramires, and Daniel F Agterberg, “Stabilizing even-parity chiral superconductivity in Sr_2RuO_4 ,” *Physical Review Research* **2**, 032023 (2020).
- [19] Aline Ramires and Manfred Sigrist, “Superconducting order parameter of Sr_2RuO_4 : A microscopic perspective,” *Physical Review B* **100**, 104501 (2019).
- [20] Steven Allan Kivelson, Andrew Chang Yuan, Brad Ramshaw, and Ronny Thomale, “A proposal for reconciling diverse experiments on the superconducting state in Sr_2RuO_4 ,” *npj Quantum Materials* **5**, 1–8 (2020).
- [21] Andrew C. Yuan, Erez Berg, and Steven A. Kivelson, “Strain-induced time reversal breaking and half quantum vortices near a putative superconducting tetracritical point in Sr_2RuO_4 ,” *Phys. Rev. B* **104**, 054518 (2021).
- [22] Astrid T Rømer, Andreas Kreisel, Marvin A Müller, PJ Hirschfeld, Ilya M Eremin, and Brian M Andersen, “Theory of strain-induced magnetic order and splitting of T_c and T_{trsb} in Sr_2RuO_4 ,” *Physical Review B* **102**, 054506 (2020).
- [23] Astrid T Rømer, PJ Hirschfeld, and Brian M Andersen, “Superconducting state of Sr_2RuO_4 in the presence of longer-range Coulomb interactions,” arXiv preprint arXiv:2101.06972 (2021).
- [24] Vadim Grinenko, Shreenanda Ghosh, Rajib Sarkar, Jean-Christophe Orain, Artem Nikitin, Matthias Elender, Debarchan Das, Zurab Guguchia, Felix Brückner, Mark E Barber, *et al.*, “Split superconducting and time-reversal symmetry-breaking transitions in Sr_2RuO_4 under stress,” *Nature Physics*, 1–7 (2021).
- [25] Jing Xia, Yoshiteru Maeno, Peter T Beyersdorf, MM Fejer, and Aharon Kapitulnik, “High resolution polar Kerr effect measurements of Sr_2RuO_4 : Evidence for broken time-reversal symmetry in the superconducting state,” *Physical review letters* **97**, 167002 (2006).
- [26] Elena Hassinger, Patrick Bourgeois-Hope, Haruka Taniguchi, S René de Cotret, Gael Grissonnanche, M Shahbaz Anwar, Yoshiteru Maeno, Nicolas Doiron-Leyraud, and Louis Taillefer, “Vertical line nodes in the superconducting gap structure of Sr_2RuO_4 ,” *Physical Review X* **7**, 011032 (2017).
- [27] Veronika Sunko, Edgar Abarca Morales, Igor Marković, Mark E Barber, Dijana Milosavljević, Federico Mazzola, Dmitry A Sokolov, Naoki Kikugawa, Cephise Cacho, Pavel Dudin, *et al.*, “Direct observation of a uniaxial stress-driven Lifshitz transition in Sr_2RuO_4 ,” *npj Quantum Materials* **4**, 1–7 (2019).
- [28] Yi-Ting Hsu, Weejee Cho, Alejandro Federico Rebola, Bulat Burganov, Carolina Adamo, Kyle M Shen, Darrell G Schlom, Craig J Fennie, and Eun-Ah Kim, “Manipulating superconductivity in ruthenates through Fermi surface engineering,” *Physical Review B* **94**, 045118 (2016).
- [29] Fabian Jerzembeck, Henrik S Røising, Alexander Steppke, Helge Rosner, Dmitry A Sokolov, Naoki Kikugawa, Thomas Scaffidi, Steven H Simon, Andrew P Mackenzie, and Clifford W Hicks, “The superconductivity of Sr_2RuO_4 under c -axis uniaxial stress,” *Nature Communications* **13**, 1–11 (2022).
- [30] It should be noted that due to \mathcal{M}_z symmetry, there exists no hybridization between the x, z -bands and y, z -bands, i.e., $\varepsilon_{x,z} = \varepsilon_{y,z} = 0$. However, in a full 3D model, such hybridization terms are allowed and can give rise to gap functions between the x, z -bands and y, z -bands, i.e., $\Delta_{x,z}, \Delta_{y,z} \neq 0$, even in the absence of spin-orbit coupling. Since Sr_2RuO_4 is quasi-two-dimensional, such terms can always be treated perturbatively.
- [31] E. I. Blount, “Symmetry properties of triplet superconductors,” *Phys. Rev. B* **32**, 2935–2944 (1985).
- [32] E. Berg, C-C. Chen, and S. A. Kivelson, “Stability of nodal quasiparticles in superconductors with coexisting orders,” *Phys. Rev. Lett.* **100**, 027003 (2008).
- [33] B Béri, “Topologically stable gapless phases of time-reversal-invariant superconductors,” *Physical Review B* **81**, 134515 (2010).
- [34] Shingo Kobayashi, Ken Shiozaki, Yukio Tanaka, and Masatoshi Sato, “Topological blount’s theorem of odd-parity superconductors,” *Phys. Rev. B* **90**, 024516 (2014).
- [35] Andreas P Schnyder, Shinsei Ryu, Akira Furusaki, and Andreas WW Ludwig, “Classification of topological insulators and superconductors in three spatial dimensions,” *Physical Review B* **78**, 195125 (2008).
- [36] By symmetry, it’s possible that $V_{x,x}(\mathbf{q}) \neq V_{y,y}(\mathbf{q})$ and $V_{x,z}(\mathbf{q}) \neq V_{y,z}(\mathbf{q})$. However, the differences $(V_{x,x} - V_{y,y})(\mathbf{q})$ and $(V_{x,z} - V_{y,z})(\mathbf{q})$ must satisfy B_{1g} symmetry with respect to \mathbf{q} . Therefore, up to $R \leq 2$ harmonics, the interactions can only mix s and $d_{x^2-y^2}$ wave harmonics, e.g., $(V_{x,x} - V_{y,y})(\mathbf{k} - \mathbf{k}') = s_1(\mathbf{k})d_1(\mathbf{k}') + d_1(\mathbf{k})s_1(\mathbf{k}') + \dots$ where \dots represent higher harmonics $R \geq 2$ or odd-parity harmonics, and thus have no direct effect on the $R = 2$ harmonics involving the d_{xy} or g -waves.
- [37] Thomas Scaffidi, Jesper C Romers, and Steven H Simon, “Pairing symmetry and dominant band in Sr_2RuO_4 ,” *Physical Review B* **89**, 220510 (2014).
- [38] DF Agterberg, TM Rice, and M Sigrist, “Orbital dependent superconductivity in Sr_2RuO_4 ,” *Physical review letters* **78**, 3374 (1997).
- [39] S Raghu, A Kapitulnik, and SA Kivelson, “Hidden quasi-one-dimensional superconductivity in Sr_2RuO_4 ,” *Physical review letters* **105**, 136401 (2010).
- [40] Jia-Wei Huo, Thomas M Rice, and Fu-Chun Zhang, “Spin density wave fluctuations and p-wave pairing in Sr_2RuO_4 ,” *Physical Review Letters* **110**, 167003 (2013).
- [41] I. A. Firmo, S. Lederer, C. Lupien, A. P. Mackenzie, J. C. Davis, and S. A. Kivelson, “Evidence from tunneling spectroscopy for a quasi-one-dimensional origin of superconductivity in Sr_2RuO_4 ,” *Phys. Rev. B* **88**, 134521 (2013).
- [42] Xin Wang, Zhiqiang Wang, and Catherine Kallin, “Higher angular momentum pairing states in Sr

- 2 RuO₄ in the presence of longer-range interactions,” arXiv preprint arXiv:2207.11180 (2022).
- [43] Bulat Burganov, Carolina Adamo, Andrew Mulder, M Uchida, PDC King, JW Harter, DE Shai, AS Gibbs, AP Mackenzie, Reinhard Uecker, *et al.*, “Strain control of fermiology and many-body interactions in two-dimensional ruthenates,” *Physical review letters* **116**, 197003 (2016).
- [44] Tosio Kato, *Perturbation theory for linear operators*, Vol. 132 (Springer Science & Business Media, 2013).
- [45] Peter D Hislop and Israel Michael Sigal, *Introduction to spectral theory: With applications to Schrödinger operators*, Vol. 113 (Springer Science & Business Media, 2012).
- [46] Volker Bach, Elliott H Lieb, and Jan Philip Solovej, “Generalized Hartree-Fock theory and the Hubbard model,” *Journal of statistical physics* **76**, 3–89 (1994).
- [47] Johnpierre Paglione, C Lupien, WA MacFarlane, JM Perz, Louis Taillefer, ZQ Mao, and Y Maeno, “Elastic tensor of Sr₂RuO₄,” *Physical Review B* **65**, 220506 (2002).
- [48] Notice that the magnitudes α are slightly different from the SI of reference [12]. Indeed, the reference only considered the single γ band case and did not modify the chemical potential μ_z , which we believe to be the main source of A_1 strain since it first appears as an onsite hopping term.

V. APPENDIX

A. Band structure

The normal state dispersion values used in this paper are found in the Supplementary Information (SI) of Ref. [43]. We repeat them here for completeness, i.e.,

$$\varepsilon_{x/y}(\mathbf{k}) = -\mu_0 - 2t_x \cos k_{x/y} - 2t_y \cos k_{y/x} \quad (16)$$

$$\varepsilon_z(\mathbf{k}) = -\mu_z - 2t_z(\cos k_x + \cos k_y) - 2t'_z(2 \cos k_x \cos k_y) \quad (17)$$

$$\varepsilon_h(\mathbf{k}) = 4t_h \sin k_x \sin k_y \quad (18)$$

Where for Sr₂RuO₄, we use the values The SO coupling was taken to be $\varepsilon_{so} = 30$ meV.

t_z (meV)	t_x (meV)	t_y/t_x	t_h/t_x	μ_z/t_z	μ_x/t_x
119	165	0.08	0.13	1.48	1.08

B. Rigorous perturbative argument

Let us consider a general even-parity \mathcal{P} 3D multi-band BCS Hamiltonian $H'(\mathbb{k})$ where $\mathbb{k} = (k_x, k_y, k_z)$ (i.e., satisfies particle-hole symmetry \mathcal{C} and thus the \mathbb{k} -local symmetry $\mathcal{K} = \mathcal{P}\mathcal{C}$). We shall assume spin degree of freedom so that $H'(\mathbb{k})$ is a $4n \times 4n$ -matrix and that $H'(\mathbb{k})$ satisfies the mirror symmetries \mathcal{M}_z at $k_z = 0, \pi$ and \mathcal{M}_{xy} at $k_x = k_y$. More specifically,

1. \mathcal{M}_z is a Hermitian operator in particle-hole space which commutes with \mathcal{P}, \mathcal{C} , satisfies $\mathcal{M}_z^2 = -1$ and commutes with $H'(\mathbb{k})$ when $k_z = 0, \pi$.
2. \mathcal{M}_{xy} is a skew-Hermitian operator which commutes with \mathcal{P}, \mathcal{C} , satisfies $\mathcal{M}_{xy}^2 = -1$ and

$$\mathcal{M}_{xy} H'(\mathbb{k})|_{\Delta'(\mathbb{k})} \mathcal{M}_{xy}^\dagger = H'(\mathbb{k})|_{-\Delta'(\mathbb{k})}, \quad k_x = k_y \quad (19)$$

Where the subscript is to indicate that the mirror symmetry \mathcal{M}_{xy} maps the gap function $\Delta'(\mathbb{k}) \mapsto -\Delta'(\mathbb{k})$.

3. \mathcal{M}_z and \mathcal{M}_{xy} anti-commute.

It's easy to see that in the case of the 3-band Sr₂RuO₄ model where $\mathcal{M}_z, \mathcal{M}_{xy}$ can be explicitly computed, such properties are satisfied (see subsection (VB 1)). It's also clear that $H'(\mathbb{k})$ includes the case of a singlet-pairing $d_{x^2-y^2} + ig$ state, i.e., $H'(\mathbb{k}) = H(\mathbb{k})$ where $H(\mathbb{k})$ in Eq. (1) denotes its restriction to $k_z = 0, \pi$. Therefore, this will be our starting point in our perturbative argument.

It's worth mentioning that the mirror symmetry \mathcal{M}_{xy} maps $\Delta'(\mathbb{k}) \mapsto -\Delta'(\mathbb{k})$, but since this is a global phase, we can apply a $U(1)$ -gauge transformation $\mathcal{U} = i\tau_3$, where τ denotes the Pauli matrices in particle-hole space, so that $\tilde{\mathcal{M}}_{xy} = \mathcal{U}\mathcal{M}_{xy}$ is a Hermitian operator which satisfies $\tilde{\mathcal{M}}_{xy}^2 = +1$ and commutes with $H'(\mathbb{k})$ in the diagonal plane $k_x = k_y$. Moreover, we shall focus on the mirror symmetry across $k_x = k_y$, but the other diagonal plane $k_x = -k_y$ can be similarly reasoned.

From explicit calculations, we know that the multi-band $d_{x^2-y^2} + ig$ state $H(\mathbb{k})$ has a point node at some \mathbf{k}_* in the horizontal planes $k_z = 0, \pi$ along the diagonals $k_x = k_y$. From Theorem (V.2), it's then clear that $\dim \ker H(\mathbf{k}_*) = 4m$ for some $m \geq 1$. In the absence of other symmetries, it is generally assumed that $m = 1$ so that we can choose $\phi(\mathbf{k}_*)$ so that $\{\phi(\mathbf{k}_*)\} = (\phi(\mathbf{k}_*), \tilde{\mathcal{M}}_{xy}\phi(\mathbf{k}_*), \mathcal{K}\phi(\mathbf{k}_*), \mathcal{K}\tilde{\mathcal{M}}_{xy}\phi(\mathbf{k}_*))$ forms a basis for $\ker H(\mathbf{k}_*)$, and we shall use $P(\mathbf{k}_*)$ to denote the projection operator onto $\ker H(\mathbf{k}_*)$.

Moving away from the explicit solution \mathbf{k}_* , let us **assume that** $H'(\mathbb{k}) - H(\mathbf{k}_*)$ is small with respect to the gap of $H(\mathbf{k}_*)$ (lowest nonzero energy level of $H(\mathbf{k}_*)$ and not to be confused with the gap function $\Delta(\mathbb{k})$) so that $P'(\mathbb{k})$ can be well-defined as the projection operator onto eigenstates of $H'(\mathbb{k})$ with energies near zero (regardless of the symmetries that $H'(\mathbb{k})$ preserves) and also unitarily equivalent to $P(\mathbf{k}_*)$ as explained in subsection (V B 3). By perturbation theory, the variation of the energy values must be small and thus it's sufficient to consider the restriction of $H'(\mathbb{k})$ to $P'(\mathbb{k})$ when attempting find the zero energies of $H'(\mathbb{k})$, i.e., only eigenstates in $P'(\mathbb{k})$ have energies sufficiently close to zero.

When $k_z = 0, \pi$ and $k_x = k_y$, from Theorem (V.2), it's clear that there must exist $\phi'(\mathbf{k})$ such that $\{\phi'(\mathbf{k})\}$ forms a complete orthonormal basis for $P'(\mathbb{k})$ (though not necessarily degenerate anymore). As an analogy, $\phi'(\mathbf{k}), \mathcal{M}_{xy}\phi'(\mathbf{k})$ should be considered as “**pseudo-spins**” in particle space, while the remaining states are considered as “pseudo-spins” in hole states. Within the basis $\{\phi'(\mathbf{k})\}$, the restriction $H'(\mathbf{k})P'(\mathbf{k})$ must be of the form

$$H'(\mathbf{k})P'(\mathbf{k}) = \begin{bmatrix} \varepsilon'(\mathbf{k}) & \hat{\Delta}'(\mathbf{k}) \\ \hat{\Delta}'(\mathbf{k})^\dagger & -\varepsilon'(\mathbf{k})^T \end{bmatrix} \quad (20)$$

By \mathcal{K} symmetry, it's clear that $\hat{\Delta}'(\mathbf{k})$ must form a singlet between the pseudo-spins, i.e., under the basis $\{\phi'(\mathbf{k})\}$, the matrix $\hat{\Delta}'(\mathbf{k}) = \Delta'(\mathbf{k})(i\sigma_2)$ where $\Delta'(\mathbf{k}) \in \mathbb{C}$ and σ denotes the Pauli matrix in pseudo-spin basis. Furthermore, under the basis $\{\phi'(\mathbf{k})\}$, the mirror symmetries $\mathcal{M}_z, \mathcal{M}_{xy}$ have the matrix forms

$$\mathcal{M}_z = \begin{bmatrix} +i & & & \\ & -i & & \\ & & -i & \\ & & & +i \end{bmatrix}, \quad \tilde{\mathcal{M}}_{xy} = \begin{bmatrix} & +1 & & \\ +1 & & & \\ & & & +1 \\ & & +1 & \end{bmatrix} \quad (21)$$

Since $H'(\mathbf{k})P'(\mathbf{k})$ preserves the mirror symmetries when $k_z = 0, k_x = k_y$, explicit calculations show that $\varepsilon'(\mathbf{k}) = \varepsilon'_0(\mathbf{k})\sigma_0$ where $\varepsilon'_0(\mathbf{k}) \in \mathbb{R}$ and $\hat{\Delta}'(\mathbf{k}) = 0$. Therefore,

$$H'(\mathbf{k})P'(\mathbf{k}) = \tau_3 \otimes \varepsilon'_0(\mathbf{k})\sigma_0 \quad (22)$$

Therefore, when $k_z = 0, \pi$ and $k_x = k_y$, the perturbed Hamiltonian $H'(\mathbf{k})$ has a nodal point at \mathbf{k} if and only if $\varepsilon'_0(\mathbf{k}) = 0$. Since this a real equation on a 1D line, it's in general satisfied at a single point node \mathbf{k}'_* near \mathbf{k}_* .

Let us now consider general k_z so that mirror symmetry \mathcal{M}_z breaks down, but still remain within the diagonal plane $k_x = k_y$. It should be noted from the matrix form of $\tilde{\mathcal{M}}_{xy}$ with respect to $\{\phi'(\mathbf{k}_*)\}$ in Eq. (21) that

$$\text{tr}(\mathcal{M}_{xy}P'(\mathbf{k}_*)) = 0 \quad (23)$$

Since $\tilde{\mathcal{M}}_{xy}$ has eigenvalue ± 1 , we see that $\text{tr}(\tilde{\mathcal{M}}_{xy}P'(\mathbb{k}))$ must be an integer and thus by continuity, for sufficiently small variations $H'(\mathbb{k}) - H(\mathbf{k}_*)$, we must also have

$$\text{tr}(\tilde{\mathcal{M}}_{xy}P'(\mathbb{k})) = 0 \quad (24)$$

Since $H'(\mathbb{k})$ still preserves mirror symmetry $\tilde{\mathcal{M}}_{xy}$ in the diagonal planes and $\dim P'(\mathbb{k}) = \dim P'(\mathbf{k}_*) = 4$, we see that eigenstates of $H'(\mathbb{k})$ in $P'(\mathbb{k})$ can be divided by the eigenspaces of $\tilde{\mathcal{M}}_{xy} = \pm 1$, each of which

is of dim 2, i.e., $\dim \ker(\tilde{\mathcal{M}}_{xy} \pm 1) = 2$. Notice that \mathcal{K} commutes with $\tilde{\mathcal{M}}_{xy}$ and thus maps within each eigenspace $\tilde{\mathcal{M}}_{xy} = \pm 1$. Hence, by Lemma (V.1), there exists an orthonormal basis $\chi_{\pm}, \mathcal{K}\chi_{\pm}$ consisting of eigenstates of $H'(\mathbb{k})$ within each eigenspace $\tilde{\mathcal{M}}_{xy} = \pm 1$, respectively. Let us now define

$$\phi'(\mathbb{k}) = \frac{1}{\sqrt{2}}(\chi_+ + \chi_-) \quad (25)$$

Then it's clear that $\{\phi'(\mathbb{k})\}$ forms a complete orthonormal basis for $P'(\mathbb{k})$. We can then repeat the same argument as before, restricting to the effective 2-band Hamiltonian $H'(\mathbb{k})P'(\mathbb{k})$, but only using mirror symmetry \mathcal{M}_{xy} this time. In this case, we see that $\hat{\Delta}'(\mathbb{k}) = 0$ while $\hat{\varepsilon}'(\mathbb{k}) = \varepsilon'_0(\mathbb{k})\sigma_0 + \varepsilon'_1(\mathbb{k})\sigma_1$, or equivalently,

$$H'(\mathbb{k})P'(\mathbb{k}) = \tau_3 \otimes (\varepsilon'_0(\mathbb{k})\sigma_0 + \varepsilon'_1(\mathbb{k})\sigma_1) \quad (26)$$

Therefore, within the diagonal plane $k_x = k_y$, the perturbed Hamiltonian $H'(\mathbb{k})$ has a node if and only if $|\varepsilon'_0(\mathbb{k})| = |\varepsilon'_1(\mathbb{k})|$. Since this is a real equation in a 2D plane, it's in general satisfied by a line, and thus implies the existence of line nodes within the diagonal plane provided that $H'(\mathbb{k}) - H(\mathbf{k}_*)$ is small. Such assumption is satisfied when $H'(\mathbb{k})$ describes a purely singlet $d_{x^2-y^2} + ig$ state which is only weakly dependent on k_z .

Once we move away from the mirror symmetries, i.e., $k_z \neq 0, \pi$ and $k_x \neq k_y$, a similar argument can be repeated to show that there exists a complete basis $\{\phi'(\mathbb{k}), \chi'(\mathbb{k}), \mathcal{K}\phi'(\mathbb{k}), \mathcal{K}\chi'(\mathbb{k})\}$ for $P'(\mathbb{k})$, where $\phi'(\mathbb{k}), \chi'(\mathbb{k})$ are not related by mirror symmetry \mathcal{M}_{xy} anymore. However, since \mathcal{K} is still preserved, the effective 2-band gap function $\hat{\Delta}'(\mathbb{k})$ must form a singlet between the pseudospins, i.e., $\hat{\Delta}'(\mathbb{k}) = \Delta'(\mathbb{k})(i\sigma_2)$. This implies that the particle-hole dispersion relation $\hat{\varepsilon}'(\mathbb{k})$ can be unitarily transformed via any $SU(2)$ rotation in pseudospin space without affecting the gap function. Therefore, the effective 2-band Hamiltonian $H'_{\text{eff}}(\mathbb{k})$ can be unitarily transformed so that $\hat{\varepsilon}'(\mathbb{k})$ is diagonal with entries $\varepsilon'_{\pm}(\mathbb{k})$, i.e.,

$$H'_{\text{eff}}(\mathbb{k}) = \left(\begin{array}{cc|cc} \varepsilon'_+(\mathbb{k}) & & & \Delta'(\mathbb{k}) \\ & \varepsilon'_-(\mathbb{k}) & -\Delta'(\mathbb{k}) & \\ \hline & -\Delta'(\mathbb{k})^* & -\varepsilon'_+(\mathbb{k}) & \\ \Delta'(\mathbb{k})^* & & & -\varepsilon'_-(\mathbb{k}) \end{array} \right) \quad (27)$$

Where the solid lines divide the particle/hole subspaces. Therefore, the effective Hamiltonian $H'_{\text{eff}}(\mathbb{k})$ has a zero mode if and only

$$|\Delta'(\mathbb{k})|^2 + \varepsilon'_+(\mathbb{k})\varepsilon'_-(\mathbb{k}) = 0 \quad (28)$$

In the absence of mirror symmetries and TRS, a small Zeeman splitting occurs in pseudospin space, i.e., $\varepsilon'_+(\mathbb{k}) \neq \varepsilon'_-(\mathbb{k})$, and thus a Bogoliubov FS is generated where Eq. (28) is satisfied.

1. Example with 3-Band Sr_2RuO_4

In the particular case of the 3-band Sr_2RuO_4 model, let

$$M_z = \exp\left(-i\frac{\pi}{2}\sigma_3\right) \otimes \begin{bmatrix} -1 & & \\ & -1 & \\ & & +1 \end{bmatrix} \quad (29)$$

$$M_{xy} = \exp\left(-i\frac{\pi}{2}(\hat{n} \cdot \vec{\sigma})\right) \otimes \begin{bmatrix} & +1 & \\ +1 & & \\ & & +1 \end{bmatrix}, \quad \hat{n} = \frac{1}{\sqrt{2}}(-1, 1, 0) \quad (30)$$

Where the first term denotes rotation in spin-basis \uparrow, \downarrow , while the second term represents the transform in orbital basis $\nu = x, y, z$ (i.e., the d_{xz}, d_{yz}, d_{xy} orbitals). With slight abuse of notation, also let M_z, M_{xy} denote the transform on the wave vector \mathbb{k} , i.e.,

$$M_z\mathbb{k} = (k_x, k_y, -k_z), \quad M_{xy}\mathbb{k} = (k_y, k_x, k_z) \quad (31)$$

Then the symmetries $\mathcal{M}_z, \mathcal{M}_{xy}$ act on $H'(\mathbb{k})$ via

$$\mathcal{M}_z H'(\mathbb{k}) \mathcal{M}_z^\dagger = \begin{bmatrix} \mathcal{M}_z & \\ & \mathcal{M}_z^* \end{bmatrix} H'(M_z^{-1}\mathbb{k}) \begin{bmatrix} \mathcal{M}_z^\dagger & \\ & \mathcal{M}_z^T \end{bmatrix} \quad (32)$$

$$\mathcal{M}_{xy} H'(\mathbb{k}) \mathcal{M}_{xy}^\dagger = \begin{bmatrix} \mathcal{M}_{xy} & \\ & \mathcal{M}_{xy}^* \end{bmatrix} H'(M_{xy}^{-1}\mathbb{k}) \begin{bmatrix} \mathcal{M}_{xy}^\dagger & \\ & \mathcal{M}_{xy}^T \end{bmatrix} \quad (33)$$

Where the block-matrix form denotes particle-hole space.

2. Exact statements regarding symmetries

Lemma V.1. *Let A be a Hermitian operator on a $2N$ -dimensional Hilbert space and \mathcal{T} be an anti-unitary operator which anti-commutes with A and satisfies $\mathcal{T} = \mathcal{T}^\dagger = \mathcal{T}^{-1}$. Then there exists an orthonormal basis of the form $\phi_i, \mathcal{T}\phi_i, i = 1, 2, \dots, N$ where ϕ_i corresponds to eigenvalue a_i and $\mathcal{T}\phi_i$ corresponds to eigenvalue $-a_i$. In particular,*

$$\dim \ker A \in 2\mathbb{N} \quad (34)$$

Proof. It's clear that if ϕ is an eigenstate of eigenvalue a , then $\mathcal{T}\phi$ is an eigenstate of eigenvalue $-a$. Therefore, if $a \neq 0$, then $\phi, \mathcal{T}\phi$ must be orthogonal, and thus the summation of all eigenspaces with nonzero eigenvalue $a \neq 0$ must be of even dimension. Since the total Hilbert space is $2N$ -dimensions, we see that $\dim \ker A \in 2\mathbb{N}$.

Let us now consider the restriction \mathcal{T}_A of \mathcal{T} to $\ker A$. Since $\mathcal{T}_A^2 = I_A$ is the identity operator on $\ker A$, we see that $(\mathcal{T}_A - I_A)(\mathcal{T}_A + I_A) = 0$. Hence, if $\phi \in \ker A$, then either $\tilde{\phi} \equiv (\mathcal{T}_A + I_A)\phi$ is nonzero and thus an eigenstate of \mathcal{T}_A with eigenvalue $+1$, OR $\tilde{\phi} = 0$ and thus ϕ is an eigenstate of \mathcal{T}_A with eigenvalue -1 . In the latter case, we see that $i\phi$ is an eigenstate of \mathcal{T}_A with eigenvalue $+1$ since \mathcal{T}_A is anti-linear. Hence, we can always find an orthonormal basis χ_1, \dots, χ_{2m} for $\ker A$ of eigenstates of \mathcal{T}_A with eigenvalue $+1$.

Now let us define

$$\phi_{2i-1/2i} = \frac{1}{\sqrt{2}}(\chi_{2i-1} \pm i\chi_{2i}), \quad i = 1, 2, \dots, m \quad (35)$$

Then it's clear that $\phi_{2i} = \mathcal{T}\phi_{2i-1}$ and thus we have found a basis of the form $\phi, \mathcal{T}\phi$ for $\ker A$ and consequently for the entire Hilbert space. \square

Theorem V.2. *Let $k_z = 0$ and $k_x = k_y$. Then*

$$\dim \ker H'(\mathbb{k}) = 4m, \quad m \in \mathbb{N} \quad (36)$$

More specifically, there exists an orthonormal basis for $\ker H'(\mathbb{k})$ of the form

$$\{\phi'(\mathbb{k})\} \equiv \{\phi'_i(\mathbb{k}), \tilde{\mathcal{M}}_{xy}\phi'_i(\mathbb{k}), \mathcal{K}\phi'_i(\mathbb{k}), \mathcal{K}\tilde{\mathcal{M}}_{xy}\phi'_i(\mathbb{k}) : i = 1, \dots, m\} \quad (37)$$

Proof. Since $H'(\mathbb{k})$ commutes with \mathcal{M}_z and \mathcal{M}_z is Hermitian with $\mathcal{M}_z^2 = -1$, we can decompose the particle-hole subspace into the eigenspaces of \mathcal{M}_z , i.e., $\ker(\mathcal{M}_z - i)$ and $\ker(\mathcal{M}_z + i)$. Notice that \mathcal{K} commutes with \mathcal{M}_z and since the eigenvalue of \mathcal{M}_z are imaginary, we see that \mathcal{K} is an anti-unitary operator between the eigenspaces $\ker(\mathcal{M}_z - i) \leftrightarrow \ker(\mathcal{M}_z + i)$. In particular, we see that $\dim \ker(\mathcal{M}_z \pm i) = 2n$

Since $H'(\mathbb{k})$ anti-commutes with \mathcal{K} , we see that if ϕ is an eigenstate of $H'(\mathbb{k})$ in $\ker(\mathcal{M}_z - i)$ with energy E , then $\mathcal{K}\phi$ is an orthogonal eigenstate of $H'(\mathbb{k})$ in $\ker(\mathcal{M}_z + i)$ with energy $-E$, and vice-versa. Similarly, notice that $\tilde{\mathcal{M}}_{xy}$ anti-commutes with \mathcal{M}_z and thus is a unitary operator which maps between the eigenspaces $\ker(\mathcal{M}_z - i) \leftrightarrow \ker(\mathcal{M}_z + i)$. Therefore, $\mathcal{K}\tilde{\mathcal{M}}_{xy}$ is an anti-unitary map which maps each eigenspace onto itself, i.e., $\ker(\mathcal{M}_z \pm i)$ is invariant under $\mathcal{K}\tilde{\mathcal{M}}_{xy}$. Notice that $\mathcal{K}\tilde{\mathcal{M}}_{xy}$ is an anti-unitary Hermitian operator which anti-commutes with $H'(\mathbb{k})$ within each eigenspace $\ker(\mathcal{M}_z \pm i)$. Therefore, by Lemma (V.1), within each eigenspace $\ker(\mathcal{M}_z \pm i)$, the kernel of $H'(\mathbb{k})$ is doubly degenerate. In fact, we can find an orthonormal basis of the form $\phi'_i, \mathcal{K}\tilde{\mathcal{M}}_{xy}\phi'_i, i = 1, \dots, m$ for $\ker H'(\mathbb{k}) \cap \ker(\mathcal{M}_z - i)$ (notice that the basis may be empty, i.e., $m = 0$, if \mathbb{k} is not a nodal point of $H'(\mathbb{k})$). And by \mathcal{K} symmetry, we see that the kernel of $H'(\mathbb{k})$ is quartic-degenerate. More specifically, $\phi'_i, \mathcal{M}_{xy}\phi'_i, \mathcal{K}\phi'_i, \mathcal{K}\tilde{\mathcal{M}}_{xy}\phi'_i$ with $i = 1, \dots, m$ form an orthonormal basis for $\ker H'(\mathbb{k})$. \square

3. The Riesz Projector and perturbation theory

For this section, let H_0 be a Hermitian operator on a finite N -dimensional Hilbert space and let $H_\lambda = H_0 + \lambda V$ denote the perturbed Hermitian operator parametrized by the small parameter λ and the perturbation is denoted by V . To have a controlled perturbation theory, we require the eigenspaces of H_0 to “evolve smoothly” to those of H_λ as we tune the small parameter λ . One way of defining such a smooth evolution rigorously is to apply the Riesz projector [44, 45], which we shall define shortly.

For simplicity, let $E^1(H_\lambda) \leq E^2(H_\lambda) \leq \dots \leq E^N(H_\lambda)$ denote the eigen-energies of H_λ in ascending order (where each energy level is repeated by their degeneracy), and let E_0 denote a (possibly degenerate) eigen-energy of H_0 , i.e., there exists some i such that

$$E^{i-1}(H_0) < E_0 \equiv E^i(H_0) = E^{i+1}(H_\lambda) \dots = E^{i+m-1}(H_0) < E^{i+m}(H_0) \quad (38)$$

It’s then clear that we can draw a circle Γ in the complex plane \mathbb{C} which only contains E_0 in the interior and none of the remaining energy levels of H_0 . By the Weyl-inequality, we know that $|E^n(H_\lambda) - E^n(H_0)| \leq |\lambda| \|V\|$, i.e., the variation in energy levels is controlled by the small parameter λ . Therefore, for sufficiently small λ , the energies $E^i(H_\lambda), \dots, E^{i+m-1}(H_\lambda)$ are still contained in the interior of Γ while the remaining energy levels of H_λ are in the exterior. Within this neighborhood of λ values, we can define the **Riesz projector** as

$$P_\lambda \equiv \frac{1}{2\pi i} \oint_\Gamma \frac{dz}{z - H_\lambda} \quad (39)$$

It’s then easy to see that P_λ is smooth with respect to λ and is equal to the projection operator onto the summation of eigenspaces $E^i(H_\lambda), \dots, E^{i+m-1}(H_\lambda)$. Since the number of energy levels (repeated by their degeneracy) does not change in the interior of Γ for sufficiently small λ , we see that $\dim P_\lambda$ is constant and $P_\lambda, P_{\lambda'}$ are unitarily equivalent for distinct values of small λ, λ' .

C. Decomposition of the interaction

Consider the interaction \mathcal{V} in Eq. (13) given by the form $V(\mathbf{k} - \mathbf{k}')$ where we have suppressed the band indices μ, μ' for simplicity. Since $V(\mathbf{q})$ is assumed to be D_4 -invariant, we can rewrite it in terms of s -wave lattice harmonics with range $R \geq 0$,

$$V(\mathbf{q}) = \sum_{R \geq 0} v(R) s_R(\mathbf{q}) \quad (40)$$

Let $|\mathbf{r}\rangle$ denote the Dirac delta function at real space lattice site \mathbf{r} and W_R denote the D_4 -invariant subspace spanned by $|\mathbf{r}\rangle$ over all lattice sites \mathbf{r} of range R , i.e., $|\mathbf{r}| = R$. Then in real space, the lattice harmonic s_R can be written as the summation over all lattice sites \mathbf{r} of range R , i.e.

$$s_R = \frac{1}{\sqrt{|W_R|}} \sum_{|\mathbf{r}|=R} |\mathbf{r}\rangle \quad (41)$$

$$s_R(\mathbf{r}) = \frac{1}{\sqrt{|W_R|}} \delta_{|\mathbf{r}|=R} \quad (42)$$

Where $|W_R|$ is the number of lattice sites \mathbf{r} with range R . Conversely, in momentum k -space, the lattice harmonic can be rewritten as

$$s_R(\mathbf{k} - \mathbf{k}') = \frac{1}{\sqrt{|W_R|}} \sum_{|\mathbf{r}|=R} \langle \mathbf{k} - \mathbf{k}' | \mathbf{r} \rangle \quad (43)$$

$$= \frac{1}{\sqrt{|W_R|}} \sum_{|\mathbf{r}|=R} \langle \mathbf{k} | \mathbf{r} \rangle \langle \mathbf{r} | \mathbf{k}' \rangle \quad (44)$$

$$= \frac{1}{\sqrt{|W_R|}} \langle \mathbf{k} | \left[\sum_{|\mathbf{r}|=R} |\mathbf{r}\rangle \langle \mathbf{r}| \right] | \mathbf{k}' \rangle \quad (45)$$

$$= \frac{1}{\sqrt{|W_R|}} \langle \mathbf{k} | P_R | \mathbf{k}' \rangle \quad (46)$$

$$(47)$$

Where P_R denotes the projection operator onto W_R . Notice that for a given range R , the subspace W_R can be decomposed into a unique combination of irreps of the symmetry group D_4 , and thus P_R must be diagonal in terms of its decomposition, i.e.,

$$P_R = \frac{1}{\sqrt{|W_R|}} \sum_{\psi_R} |\psi_R\rangle \langle \psi_R| \quad (48)$$

Where the summation is over all possible lattice harmonics ψ_R in W_R corresponding to distinct irreps. In particular,

$$s_R(\mathbf{k} - \mathbf{k}') = \langle \mathbf{k} | P_R | \mathbf{k}' \rangle = \frac{1}{\sqrt{|W_R|}} \sum_{\psi_R} \psi_R(\mathbf{k}) \psi_R(\mathbf{k}')^* \quad (49)$$

As an example, consider the case $R = 1$ in Table II. Since only $W_1 = A_1 \oplus B_1 \oplus E$, we see that

$$s_1(\mathbf{k} - \mathbf{k}') = \frac{1}{2} (s_1(\mathbf{k})s_1(\mathbf{k}') + d_1(\mathbf{k})d_1(\mathbf{k}')) + \frac{1}{2} (p_x(\mathbf{k})p_x(\mathbf{k}') + p_y(\mathbf{k})p_y(\mathbf{k}')) \quad (50)$$

Where $p_x(\mathbf{k}), p_y(\mathbf{k})$ is an orthonormal basis for the E irrep in W_1 . Notice that the terms projecting into the E irrep are not involved in computing the nonlinear gap equation in Eq. (15) since we assumed that the gap function Δ is of even parity. Therefore, in the main text, lattice harmonics belonging to the E irrep for any range R are omitted.

D. Diagonalization of 2-band BCS Hamiltonian: $SU(4) \rightarrow SO(6)$

1. Setup

Ignoring spin-orbit coupling, $\varepsilon_{\text{so}}(\mathbf{k}) = 0$, the 2-band system involving the α, β -bands decouples from the single γ band in the BCS Hamiltonian. Therefore, we can use the reduced 2-band Nambu spinor (in contrast to the 3-band spinor in Eq. (2)),

$$\Psi^\dagger(\mathbf{k}) = \left[\psi_{x\uparrow}^\dagger(\mathbf{k}) \quad \psi_{y\uparrow}^\dagger(\mathbf{k}) \mid -\psi_{x\downarrow}(-\mathbf{k}) \quad -\psi_{y\downarrow}(-\mathbf{k}) \right] \quad (51)$$

To rewrite the decoupled 2-band BCS Hamiltonian.

$$H(\mathbf{k}) = \left(\begin{array}{cc|cc} \varepsilon_x & \varepsilon_h & \Delta_x & \Delta_h \\ \varepsilon_h & \varepsilon_y & \Delta_h & \Delta_y \\ \hline \Delta_x^\dagger & \Delta_h^\dagger & -\varepsilon_x & -\varepsilon_h \\ \Delta_h^\dagger & \Delta_y^\dagger & -\varepsilon_h & -\varepsilon_y \end{array} \right) \quad (52)$$

Where we have kept the \mathbf{k} -dependency implicit in the entries since the BCS Hamiltonian $H(\mathbf{k})$ is local in \mathbf{k} , and the solid lines separate the particle-hole subspaces. Due to particle-hole symmetry and even parity, the eigen-energies of the local $H(\mathbf{k})$ is doubly degenerate, i.e., of the form $\pm E$. To reduce this degeneracy and make the diagonalization process more transparent, let us consider $H(\mathbf{k})^2$, i.e.,

$$H(\mathbf{k})^2 = \left(\begin{array}{cc|cc} R+h & a+ib & 0 & c+id \\ a-ib & R-h & -c-id & 0 \\ \hline 0 & -c+id & R+h & a-ib \\ c-id & 0 & a+ib & R-h \end{array} \right) \quad (53)$$

$$= R + h\sigma_{03} + a\sigma_{01} - b\sigma_{32} - c\sigma_{22} - d\sigma_{12} \quad (54)$$

Where $\sigma_{\mu\nu} = \sigma_\mu \otimes \sigma_\nu$ is the tensor product of Pauli matrices and

$$R = \varepsilon_h^2 + |\Delta_h|^2 + \frac{1}{2} (\varepsilon_x^2 + |\Delta_x|^2 + \varepsilon_y^2 + |\Delta_y|^2) \quad (55)$$

$$h = \frac{1}{2} (\varepsilon_x^2 + |\Delta_x|^2 - \varepsilon_y^2 - |\Delta_y|^2) \quad (56)$$

$$a + ib = \Delta_h^\dagger \Delta_x + \Delta_h \Delta_y^\dagger + \varepsilon_h (\varepsilon_x + \varepsilon_y) \quad (57)$$

$$c + id = \Delta_h (\varepsilon_x - \varepsilon_y) - (\Delta_x - \Delta_y) \varepsilon_h \quad (58)$$

Indeed, to solve the nonlinear gap equation, we need to obtain the 1-particle density matrix (1-pdm) $\Gamma(\mathbf{k})$ [46] defined by

$$\Gamma(\mathbf{k}) \equiv \frac{1}{e^{\beta H(\mathbf{k})} + 1} \quad (59)$$

$$= \frac{1}{2} - H(\mathbf{k})U(\mathbf{k})^\dagger \frac{1}{2|\mathcal{E}(\mathbf{k})|} \tanh\left(\frac{\beta|\mathcal{E}(\mathbf{k})|}{2}\right) U(\mathbf{k}) \quad (60)$$

Where $U(\mathbf{k})$ is the unitary matrix which diagonalizes $H(\mathbf{k})^2$ into $\mathcal{E}(k)^2$. Notice that the 1-pdm $\Gamma(k)$ is related to the Nambu spinors in Eq. (51) in the sense that the matrix entries of $\Gamma(\mathbf{k})$ are given by

$$\Gamma(\mathbf{k})_{ab} = \langle \Psi^\dagger(\mathbf{k})_b \Psi(\mathbf{k})_a \rangle \quad (61)$$

2. A reformulation of $SU(2) \rightarrow SO(3)$

The single-band BCS Hamiltonian is generally diagonalized via the $SU(2) \rightarrow SO(3)$ relation (or $\mathfrak{su}(2) \leftrightarrow \mathfrak{so}(3)$ isomorphism) and thus it is natural to think the corresponding $SU(4) \rightarrow SO(6)$ homomorphism ($\mathfrak{su}(4) \leftrightarrow \mathfrak{so}(6)$) can be used to diagonalize the 2-band BCS Hamiltonian. With that in mind, let us reformulate the $SU(2) \rightarrow SO(3)$ relation so that it can be easily generalized to the $SU(4) \rightarrow SO(6)$ isomorphism.

Let $\hat{a} \wedge \hat{b}$ be the anti-symmetric matrix with entry -1 at (a, b) and $+1$ as (b, a) . In the example of $d = 3$ dimensions,

$$\hat{1} \wedge \hat{2} = -iL_3 \quad (62)$$

$$\exp(\theta \hat{1} \wedge \hat{2}) = \exp(-i\theta L_3) \quad (63)$$

Where L_3 is the standard angular momentum along the $\hat{3}$ direction. Notice that in $d = 3$ dimension, a rotation in a plan (e.g., $e^{-i\theta L_3}$) can be specified by the normal vector $\hat{3}$ and a rotation angle θ . However, in higher dimensions, this is impossible and thus we instead specify a rotation by the plane, e.g., $\hat{1} \wedge \hat{2}$ (the plane spanned by the orthonormal frame $\hat{1}, \hat{2}$), and the rotation angle θ . Notice that $\hat{1} \wedge \hat{2} = -\hat{2} \wedge \hat{1}$, and thus the order of the 2 axes represent the direction of rotation, e.g., $\exp(\theta \hat{1} \wedge \hat{2})$ rotates the axes $\hat{1} \rightarrow \hat{2}$ by an angle of θ .

It's then clear that the $SU(2) \rightarrow SO(3)$ relation ($\mathfrak{su}(2) \leftrightarrow \mathfrak{so}(3)$ isomorphism) is given by

$$\frac{1}{2i}\sigma_1 \leftrightarrow \hat{2} \wedge \hat{3} \quad (64)$$

$$\frac{1}{2i}\sigma_2 \leftrightarrow \hat{3} \wedge \hat{1} \quad (65)$$

$$\frac{1}{2i}\sigma_3 \leftrightarrow \hat{1} \wedge \hat{2} \quad (66)$$

Where σ_i are the Pauli matrices. In particular, a 2×2 Hermitian matrix in the Lie algebra $isu(2)$

$$H = \cos \theta \sigma_3 + \sin \theta \sigma_1 \leftrightarrow \cos \theta \hat{1} \wedge \hat{2} + \sin \theta \hat{2} \wedge \hat{3} \quad (67)$$

Can be diagonalized $H = U^\dagger \sigma_3 U$ via the unitary operator

$$U = \exp\left(-\theta \frac{\sigma_2}{2i}\right) \leftrightarrow \exp(\theta \hat{3} \wedge \hat{1}) \quad (68)$$

It should be emphasized that the only requirement for such a diagonalization procedure is that $\hat{1}, \hat{2}, \hat{3}$ form an orthonormal frame. In higher dimensions, such an orthonormal frame may be arbitrarily chosen, and may not correspond to the original standard axes.

3. The $SU(4) \rightarrow SO(6)$ Relation and its Application to the 2-band System

	0	1	2	3
0		$2 \wedge 3$	$\hat{3} \wedge \hat{1}$	$1 \wedge 2$
1	$\hat{2}' \wedge \hat{3}'$	$\hat{1}' \wedge \hat{1}$	$1' \wedge 2$	$\hat{1}' \wedge \hat{3}$
2	$\hat{3}' \wedge \hat{1}'$	$\hat{2}' \wedge \hat{1}$	$\hat{2}' \wedge \hat{2}$	$\hat{2}' \wedge \hat{3}$
3	$\hat{1}' \wedge \hat{2}'$	$\hat{3}' \wedge \hat{1}$	$\hat{3}' \wedge \hat{2}$	$\hat{3}' \wedge \hat{3}$

(69)

TABLE IV. $SU(4) \rightarrow SO(6)$ Relation. $\hat{1}, \hat{2}, \hat{3}, \hat{1}', \hat{2}', \hat{3}'$ denote the 6-axes generating \mathbb{R}^6 so that $\hat{a} \wedge \hat{b}$ generates the Lie algebra $\mathfrak{so}(6)$. The entry $\hat{a} \wedge \hat{b}$ in row μ and column ν corresponds to $\sigma_{\mu\nu}/2i$ where $\sigma_{\mu\nu} = \sigma_\mu \otimes \sigma_\nu$ is the tensor product of Pauli matrices, e.g., $\sigma_{13}/2i \leftrightarrow \hat{1}' \wedge \hat{3}$. The red box show the only nonzero entries in $H(\mathbf{k})^2$ in Eq. (54).

Using the framework established in the previous section, we can easily generalize the isomorphism to $SU(4) \rightarrow SO(6)$, tabulated in Table. VD3. Indeed, let $\hat{1}, \hat{2}, \hat{3}, \hat{1}', \hat{2}', \hat{3}'$ denote the 6-axes generating \mathbb{R}^6 so that $\hat{a} \wedge \hat{b}$ generates the Lie algebra $\mathfrak{so}(6)$. Let $\sigma_{\mu\nu} = \sigma_\mu \otimes \sigma_\nu$ denote the tensor product of Pauli matrices (all except σ_{00}) which generates the Lie algebra $isu(4)$. Then Table. VD3 is read in the following manner: the entry $\hat{a} \wedge \hat{b}$ in row μ and column ν corresponds to $\sigma_{\mu\nu}/2i$, e.g., $\sigma_{13}/2i \leftrightarrow \hat{1}' \wedge \hat{3}$.

To apply this isomorphism in diagonalizing the 2-band system, notice that the red lines in Table. VD3 boxes the only entries occurring in $H(\mathbf{k})^2$ as given in Eq. (54). Therefore, we can map $H(\mathbf{k})^2$ into the Lie algebra $\mathfrak{so}(6)$ so that

$$H(\mathbf{k})^2 \leftrightarrow h \hat{1} \wedge \hat{2} + g \hat{2} \wedge \hat{3} \quad (70)$$

$$\leftrightarrow r (\cos \theta \hat{1} \wedge \hat{2} + \sin \theta \hat{2} \wedge \hat{3}) \quad (71)$$

Where we have ignored that constant R term since it commutes with any unitary operator and

$$g \hat{n} = a \hat{3} + b \hat{3}' + c \hat{2}' + d \hat{1}', \quad r^2 = h^2 + g^2 \quad (72)$$

It's then clear that $\hat{1}, \hat{2}, \hat{n}$ form an orthonormal frame in \mathbb{R}^6 , and thus using the example given in Eq. (67), it's intuitive to see that $H(\mathbf{k})^2$ is diagonalized via

$$U(\mathbf{k}) \leftrightarrow \exp(\theta \hat{n} \wedge \hat{1}) \quad (73)$$

$$= \exp\left(i \frac{\theta}{2g} (a\sigma_{02} + b\sigma_{31} + c\sigma_{21} + d\sigma_{11})\right) \quad (74)$$

$$= \cos\left(\frac{\theta}{2}\right) + i \sin\left(\frac{\theta}{2}\right) \frac{1}{g} (a\sigma_{02} + b\sigma_{31} + c\sigma_{21} + d\sigma_{11}) \quad (75)$$

So that

$$H(\mathbf{k})^2 = U(\mathbf{k})^\dagger \mathcal{E}(\mathbf{k})^2 U(\mathbf{k}), \quad \mathcal{E}(\mathbf{k})^2 = R + r\sigma_{03} \quad (76)$$

In particular, there exists $F(\mathbf{k}), f(\mathbf{k})$ given by

$$F(\mathbf{k}) = \sum_{\sigma=\pm} \frac{1}{4\sqrt{R(\mathbf{k}) + \sigma r(\mathbf{k})}} \tanh\left(\frac{\beta}{2} \sqrt{R(\mathbf{k}) + \sigma r(\mathbf{k})}\right) \quad (77)$$

$$f(\mathbf{k}) = \sum_{\sigma=\pm} \frac{\sigma}{4\sqrt{R(\mathbf{k}) + \sigma r(\mathbf{k})}} \tanh\left(\frac{\beta}{2} \sqrt{R(\mathbf{k}) + \sigma r(\mathbf{k})}\right) \quad (78)$$

Such that

$$\frac{1}{2|\mathcal{E}(\mathbf{k})|} \tanh\left(\frac{\beta|\mathcal{E}(\mathbf{k})|}{2}\right) = F(\mathbf{k}) + f(\mathbf{k})\sigma_{03} \quad (79)$$

$$U(\mathbf{k})^\dagger \frac{1}{2|\mathcal{E}(\mathbf{k})|} \tanh\left(\frac{\beta|\mathcal{E}(\mathbf{k})|}{2}\right) U(\mathbf{k}) = F(\mathbf{k}) + \frac{f(\mathbf{k})}{r(\mathbf{k})} \begin{pmatrix} h & a+ib & 0 & c+id \\ a-ib & -h & -c-id & 0 \\ 0 & -c+id & +h & a-ib \\ c-id & 0 & a+ib & -h \end{pmatrix} \quad (80)$$

$$= F(\mathbf{k}) + \frac{f(\mathbf{k})}{r(\mathbf{k})} (H(\mathbf{k})^2 - R(\mathbf{k})) \quad (81)$$

It's then easy to obtain the 1-pdm $\Gamma(\mathbf{k})$ in Eq. (59).

E. Simulating strain and stress

In this section, we describe the detailed parameters used to simulate pure A_1 and B_2 strain in the main text. For simplicity, let us define

$$\varepsilon_0 \equiv \frac{1}{2}(\varepsilon_x + \varepsilon_y) \quad (82)$$

$$\varepsilon_3 \equiv \frac{1}{2}(\varepsilon_x - \varepsilon_y) \quad (83)$$

Where $\varepsilon_0, \varepsilon_3$ should be regarded as the coefficients of decomposing the x, y band structure into Pauli matrices, i.e.,

$$\begin{pmatrix} \varepsilon_x & \varepsilon_h \\ \varepsilon_h & \varepsilon_y \end{pmatrix} = \varepsilon_0 \sigma_0 + \varepsilon_h \sigma_1 + \varepsilon_3 \sigma_3 \quad (84)$$

In the absence of strain, $\varepsilon_x, \varepsilon_y$ are given by Eq. (16) and thus we rewritten the equations as follows

$$\varepsilon_0(\mathbf{k}) = -\mu_0 - 2t_0(\cos k_x + \cos k_y) + 4t'_0 \sin k_x \sin k_y, \quad t_0 = (t_x + t_y)/2 \quad (85)$$

$$\varepsilon_3(\mathbf{k}) = -2t_3(\cos k_x - \cos k_y) - 2t'_3(\cos k_x - \cos k_y), \quad t_3 = (t_x - t_y)/2 \quad (86)$$

$$\varepsilon_z(\mathbf{k}) = -\mu_z - 2t_z(\cos k_x + \cos k_y) - 2t'_z(2 \cos k_x \cos k_y) \quad (87)$$

$$\varepsilon_h(\mathbf{k}) = 4t_h \sin k_x \sin k_y \quad (88)$$

To simulate different types of strain, let us introduce the following notation

$$\varepsilon_0(\mathbf{k}) = -\mu_{0,A_1} - 2t_{0,A_1}(\cos k_x + \cos k_y) - 2t_{0,B_1}(\cos k_x - \cos k_y) + 4t_{0,B_2} \sin k_x \sin k_y \quad (89)$$

$$\varepsilon_3(\mathbf{k}) = -2t_{3,A_1}(\cos k_x - \cos k_y) - 2t_{3,B_1}(\cos k_x + \cos k_y) \quad (90)$$

$$\varepsilon_z(\mathbf{k}) = -\mu_{z,A_1} - 2t_{z,A_1}(\cos k_x + \cos k_y) - 2t'_{z,A_1}(2 \cos k_x \cos k_y) \quad (91)$$

$$- 2t_{z,B_1}(\cos k_x - \cos k_y) + 4t_{z,B_2} \sin k_x \sin k_y \quad (92)$$

$$\varepsilon_h(\mathbf{k}) = 4t_{h,A_1} \sin k_x \sin k_y \quad (93)$$

To simulate pure A_1 strain ε_{A_1} , we have

$$t_{s,A_1}(\varepsilon_{A_1}) = t_s(1 - \alpha_{t,A_1}\varepsilon_{A_1}), \quad s = z, z', 0, 3, h \quad (94)$$

$$\mu_{z,A_1}(\varepsilon_{A_1}) = \mu_0(1 - \alpha_{\mu,A_1}\varepsilon_{A_1}) \quad (95)$$

Where μ_{0,A_1} is modified so that the total density of electrons $\langle n \rangle$ is kept fixed for nonzero values of ε_{A_1} , and we have taken $\alpha_{t,A_1} = 3$ and $\alpha_{\mu,A_1} = 8$ so that we mainly modify the chemical potentials when simulating pure A_1 strain. Similarly, to simulate pure B_1 and B_2 strain, we have

$$t_{s,B_1}(\varepsilon_{B_1}) = -t_s\alpha_{B_1}\varepsilon_{B_1}, \quad s = z, 0, 3 \quad (96)$$

$$t_{s,B_2}(\varepsilon_{B_2}) = -t_3\alpha_{B_2}\varepsilon_{B_2}, \quad s = z, 0 \quad (97)$$

Where we have taken $\alpha_{B_1} = \alpha_{B_2} = 12$.

It should be noted that in order to simulate uniaxial stress, we used the Poisson ratio $\nu \approx 0.3935$ for Sr_2RuO_4 [47] so that both A_1 strain and B_1 strain are present, i.e.,

$$\varepsilon_{yy} = -\nu\varepsilon_{xx} \quad (98)$$

$$\varepsilon_{A_1} = \frac{1}{2}(\varepsilon_{xx} + \varepsilon_{yy}) \quad (99)$$

$$\varepsilon_{B_1} = \frac{1}{2}(\varepsilon_{xx} - \varepsilon_{yy}) \quad (100)$$

The magnitudes $\alpha_{t,A_1}, \alpha_{\mu,A_1}, \alpha_{B_1}$ were tuned [48] so that the γ band in Sr_2RuO_4 crosses the Van Hove point at $\varepsilon_{xx} \approx -0.44\%$ [12], while the α, β bands distort slightly (an asymmetry of $\sim 2\%$) [27].